博士論文

Exploration of novel mast cell-targeted preventive and therapeutic molecules for allergic disorders

（肥満細胞を標的としたアレルギー疾患の新規予防および治療分子の探索）

亀井　力哉

広島大学大学院先端物質科学研究科

2017 年 3 月

目次

１．主論文

Exploration of novel mast cell-targeted preventive and therapeutic molecules for allergic disorders
(肥満細胞を標的としたアレルギー疾患の新規予防および治療分子の探索)
亀井　力哉

２．公表論文

(1) Impact of histone H1 on the progression of allergic rhinitis and its suppression by neutralizing antibody in mice
Toshiaki Nakano, Rikiya Kamei, Takashi Fujimura, Yuki Takaoka, Ayane Hori, Chia-Yun Lai, Kuei-Chen Chiang, Yayoi Shimada, Naoya Ohmori, Takeshi Goto, Kazuhisa Ono, Chao-Long Chen, Shigeru Goto, and Seiji Kawamoto
PLoS ONE, **11** (4), e0153630 (2016) (19 pages)

(2) A flavanone derivative from the Asian medicinal herb (*Perilla frutescens*) potently suppresses IgE-mediated immediate hypersensitivity reactions
Rikiya Kamei, Takashi Fujimura, Miki Matsuda, Kotaro Kakihara, Noriko Hirakawa, Kenji Baba, Kazuhisa Ono, Kenji Arakawa, and Seiji Kawamoto
Biochemical and Biophysical Research Communications, 483, 674-679 (2017)

主論文

Contents

General introduction

1. Explosion of allergic disorders all over the world

Allergic diseases are global problem. The current prevalence rates of allergic diseases become 10-30% of people in countries of the world, and those in the developing countries dramatically go up to reach the rate of advanced countries[1]. Also in Japan, allergic patients have upsurged since the postwar era, and already reached almost a half of Japanese population. Allergic disorders bring bothersome symptoms such as sneezing, runny nose, dermatitis, fever and so on to feel fatigue and dramatically reduce patients' quality of life.

2. Pathogenic mechanism of allergic disorders, and critical roles of mast cells

2.1. Systemic immune responses

Exogenous protein antigens are primarily phagocytosed by antigen presenting cells (APCs). APCs activates T cells by presenting antigenic peptide-major histocompatibility complex (MHC) complex *via* T cell receptors, and T cells initiates antigen-specific immune responses. In such acquired immune responses, cellular immunity with cytotoxicity is regulated by type 1 helper T (Th1) cells, while humoral immunity with antigen-specific immunoglobulins produced by B cells is organized by type 2 helper T (Th2) cells. Some effector T and B cells stay in lymphoid tissues

retaining their antigen-specificity, and are survived as memory cells to quickly restart the specific immune response upon re-entry of antigens.

2.2. Proallergic factors

Th2 cells organizes allergic reactions. APCs regulates differentiation of Th cells with various soluble or membrane-binding molecules as shown in Fig. 1. Th1 differentiation is induced by interleukin-12 (IL-12) secreted by dendritic cells (DCs), while Th2 differentiation is initiated by OX40 ligand^{high} type 2 DCs (DC2), and further enhanced by DC2-derived prostaglandin E_2 (PGE_2) and Th2 cytokines (*e.g.* IL-4)[2,3].

Components of exogenous pathogens (*e.g.* lipopolysaccharide and virus RNA) and endogenous self-ligands (*e.g.* self-nucleic acids and IL-1a) are known to act as proinflammatory factors triggering innate immune responses. Those proinflammatory factors represent specific molecular patterns recognized by pattern recognition receptors (PRRs), and enhance Th cell differentiation[4]. Endogenous ligands are considered as a security alarm for host body and referred to damage-associated molecular patterns (DAMPs)[5]. DAMPs induce proallergic cytokines such as thymic stromal lymphopoietin (TSLP), IL-33 and IL-25. Those cytokines induce type 2 cytokine production from type 2 innate lymphoid cells (ILC2s) as well as activates DCs, basophils and mast cells towards preallergic conditions[6].

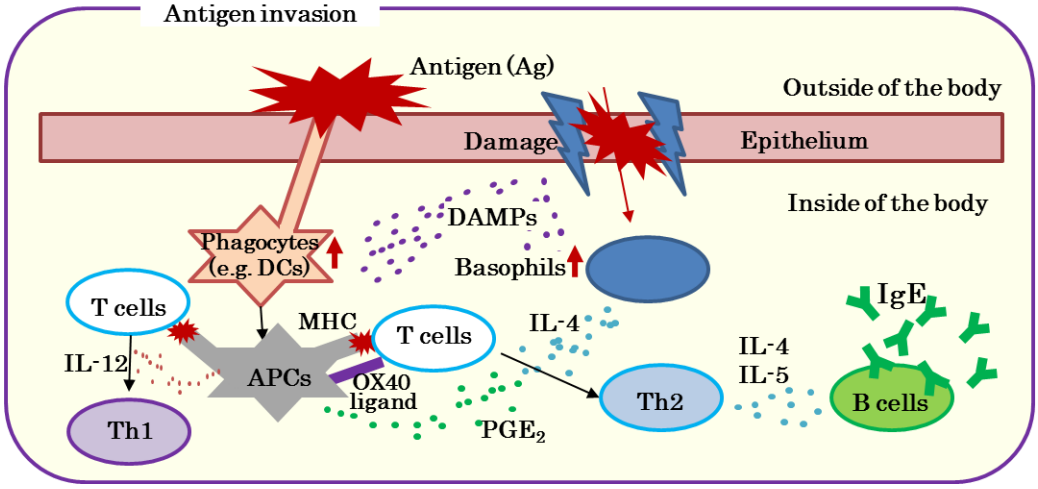

Fig. 1. Systemic immune reactions via Th2 cells upon antigen invasion

2.3. Antigen-specific IgE and mast cells play a vital role for type I allergic reaction

Immediate hypersensitivity reaction (type I allergic reaction) requires antigen-specific immunoglobulin E (IgE) and mast cell reactions[7]. The IgE antibody binds to high affinity IgE receptor (FcεRI) on mast cells, and cross-linking of IgE bound on the receptor by antigens triggers mast cell degranulation, which is known as type I allergic reaction or immediate hypersensitivity reaction. The mast cell granule contains proteases[8] (mast cell proteases, tryptase and chymase) and histamine, both of which lead to vasodilatation for infiltration of leucocytes to inflammatory sites[9,10], and stimulate nerves to develop allergic symptoms such as sneezing and itch[11]. Histamine also induces DC maturation towards DC2 with decreased IL-12 expression, which induce Th2 skewing[12]. Moreover, activated mast cells also up-regulates Th2 polarization through proallergic mediator productions (Fig.

2); IL-4 and IL-13 not only induce Th2 differentiation, but also provoke IgE-hyperproduction from B cells. PGD_2 acts as a Th2 chemoattractant as well as induces Th2 cytokines production from ILC2s[13].

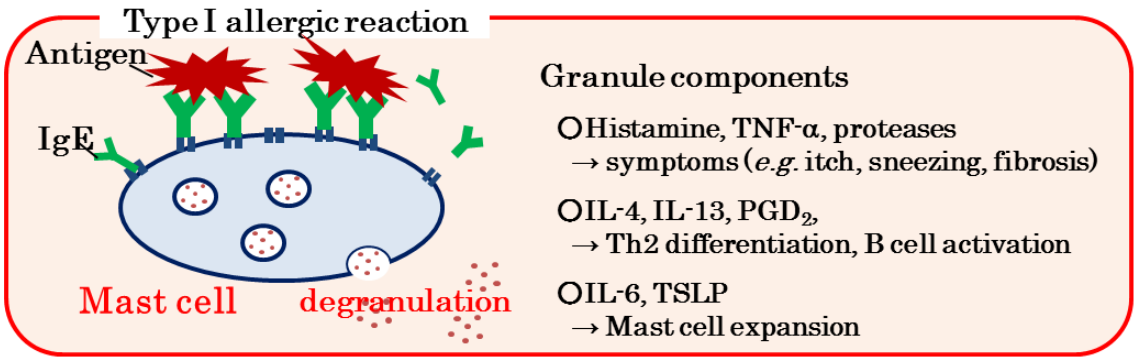

Fig. 2. IgE-mediated mast cell reaction (immediately hypersensitivity; type I allergic reaction)[14]

Mast cells are auto-activated in allergic conditions by proallergic factors. For example, TSLP, IL-25 and IL-33 are secreted from epithelial cells by allergic itch-induced scratch, and induce mast cell expansion and activation[15-19]. Additionally, activated mast cells can secrete autocrine factors. Mast cell-produced TSLP and IL-13 induces self-expansion[20]. Mast cell-derived tryptase also triggers degranulation *via* protease-activated receptor-2[21].

Several allergic models (*e.g.* allergic hypothermia model, and passive cutaneous anaphylaxis model) can explain type I allergic reaction driven by FcεRI-mediated mast cell degranulation. Those reactions are impaired in mast cell-depleted mice (Mas-TRECK mice) carrying a transgene of diphtheria toxin (DT) receptor under the control of a mast cell-specific

promoter[22]. Edema and anaphylaxis induced by some cationic drugs (*e.g.* insulin and bleomycin) are also driven by mast cell reactions[23,24].

2.4. Signal transduction leading to mast cell degranulation

Signal transduction for mast cell degranulation is initiated by cross-linking of IgE bound on FcεRI by antigens. The FcεRI signaling pathway is composed of two major independent pathways; one is a "Lyn-Syk-PLCγ pathway" to cause membrane fusion of mast cell granules for exocytosis, and another is a "Fyn-Gab2-PI3K pathway" to activate microtubule dynamics for granule translocation (Fig. 3)[25].

On the Lyn-Syk-PLCγ pathway, an FcεRI-proximal kinase Lyn is firstly auto-phosphorylated, and phosphorylates Syk, which in turn activates a downstream phosphorylation cascade including PI3K and PLCγ. PLCγ-produced $InsP_3$ leads to intracellular Ca^{2+} influx from endoplasmic reticulum (ER) *via* $InsP_3$ receptor on ER. The store-opened Ca^{2+} influx further activates calcium release-activated calcium channel (CRAC) to provoke secondary Ca^{2+} influx, that positively regulates soluble *N*-ethylmaleimide sensitive fusion protein attachment protein receptor (SNARE)-mediated exocytosis of mast cell granules[26]. On the Fyn-Gab2-PI3K pathway, another FcεRI-proximal kinase Fyn is phosphorylated by Lyn, and then downstream signaling molecules (including Gab2, PI3K and Akt) are successively phosphorylated. Akt forms a complex with DOCK5, Nck2 and GSK3β, and phosphorylates GSK3β to

promote mast cell granule translocation *via* microtubules[27].

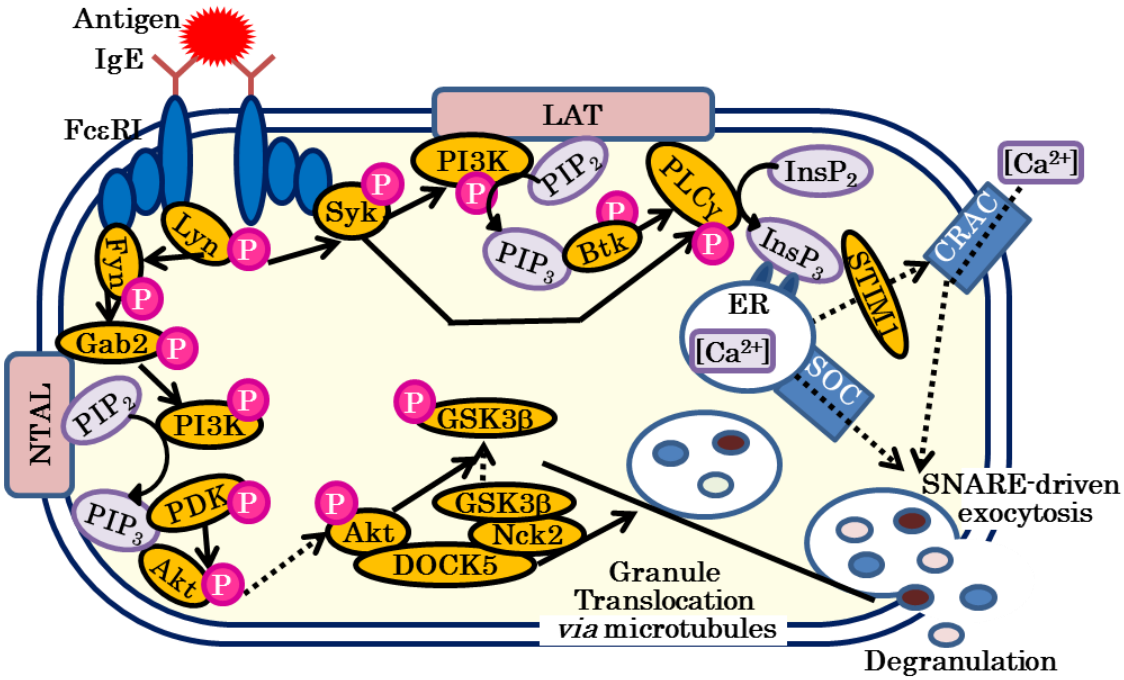

Fig. 3. FcεRI-mediated signal transduction for degranulation of mast cells
Lyn; Src family protein tyrosine kinase, Lyn, Syk; spleen tyrosine kinase, PLCγs; phospholipase Cγs, LAT; linker for activation of T cells, Fyn; Src family protein tyrosine kinase, Fyn, Gab2; GRB2-associated-binding protein 2, PI3K; phosphatidylinositol-4,5-bisphosphate 3-kinase, NTAL; non-T cell activation linker, Akt; Akt/protein kinase B (PKB), GSK3β; glycogen synthase kinase-3β, DOCK5; dedicator of cytokinesis 5, PIP_2; phosphatidylinositol-4,5-bisphosphate, PIP_3; phosphatidylinositol-3,4,5 -bisphosphate, $InsP_2$; inositol-4,5-bisphosphate, $InsP_3$; inositol-1,4,5 -trisphosphate

3. Therapeutic and preventive intervention of allergic diseases

3.1. Current therapeutic strategies for allergy and their problems

Antigen-specific immunotherapy is known as an only radical

treatment of allergic disease, and has been operated mainly in European countries and United States. In this therapy, antigen extract at lower dose than onset threshold is repeatedly injected with gradual increase in their dosages to induce antigen-specific immune-tolerance[28,29]. The tolerance is mediated by regulatory T cells (Treg) expressing IL-10 and/or transforming growth factor-β. Treg not only suppress Th2 response to decrease IgE production, but also induce immune suppressive IgG4 antibody response[30,31]. Although the efficacy of specific immune-therapy is evident, current therapy with crude antigen extract has a risk of severe side effects such as systemic anaphylaxis, and neo-sensitization with allergens. Another problem of current crude vaccine is that a profound differences in the efficacy is seen among each patient[32]. Those situations hamper allergen-specific immunotherapy to become common in Japan[33]. Instead, a major treatment of allergy is conducted by symptomatic drugs that show dramatic improvement of allergic symptoms for several hours. Their therapeutic targets, include proinflammatory mediators secreted by mast cells, IgE, and IL-5[34-37]. Those drugs have a certain effect for suppression of symptoms and improvement of patients' quality of life, but the treatment is not curable, and still has problems including a necessity of medical cost of continuing prescription and side effects. For those reasons, discovery of safer and more effective anti-allergic target molecules is highly expected.

3.2. Prevention of allergy by functional foods

Preventive medicine is aim to prevent diseases by promoting mental and physical health using knowledges about their causes and mechanisms of their pathogenesis. The traditional ideology has become important because of escalating medical costs and difficulty of radical cure in many cases. Improvement of food lifestyle is commonly recommended because high fatty and high-calorie diets are known as a reason of increasing risk of lifestyle-related diseases[38,39]. In Japan, studies on functional foods have been accelerated, and "physiologically functional food" system has been introduced by Nature magazine. In this article, some trials of Japanese functional foods are introduced, such as low-allergen rice with decreasing a risk of food allergy, and fish oils with abundant docosahexaenoic acid reducing a neutral fat value in the blood to improve the hyperlipemia[40]. For allergy prevention, mandarin orange-derived hesperidin improve allergic condition with downregulating serum specific IgE and lung Th2 cytokines in experimental asthma model mice[41]. Green tea-derived epigallocatechin gallate suppresses type I allergic reaction and improves clinical score of cedar pollinosis in humans[42]. Some strains of *Lactobacillus* improve Th1/Th2 balance in food allergy model mice and cedar pollinosis humans[43,44]. Those discoveries contributes not only to improvement of patients' symptoms, but also to the development of anti-allergic drugs.

4. Objectives of this study

In the present study, I aimed to explore novel mast cell-targeted preventive and therapeutic molecules against type I allergic disorders. In Chapters 1 and 2, I discovered endogenous histone H1 as a novel exacerbation factor of allergy, and demonstrated that this molecule is a useful therapeutic target for type I allergic disorders. In Chapter 3, I tried to isolate and identify a novel type I allergic reaction inhibitory factor from the Asian medicinal herb *Perilla frutescens*, and attempted to elucidate its mechanisms of action.

Chapter 1:

Endogenous histone H1 acts as a novel danger signal in allergy exacerbation

1. Introduction

Damage-associated molecular patterns (DAMPs) cause inflammation at internal emergency sites where proinflammatory self-ligands are released. Nucleic components usually locate in nucleus, while the components are released extracellularly when cells are dead or stressed, and subsequently act as proinflammatory factor in wound or infection sites[5]. For example, extracellular ATP is released *via* cell necrosis, apoptosis or lysosome-mediated exocytosis at inflammatory sites, and shows proinflammatory activities in infection[45]. ATP chemotactically attracts immature DCs as well as induces maturation of DC with upregulating its CD80/86 expression toward Th2 polarization[46,47]. ATP also activates cytokine production and degranulation from mast cell, moreover, activated mast cells secrete ATP by themselves[48,49].

Histones are the major proteins in nucleic compounds, and classified into linker histone H1 and core histones including H2A, H2B, H3 and H4 which respectively contribute to housing DNA and epigenetic regulation of gene expression. The new roles of extracellular histones have been successively found, such as proinflammatory activity through up-regulating cytokine production including IL-1β, IL-6, IL-8 and TNF-α from monocytes

via TLR-4 [50]. Moreover, Ronit S E, *et al.* (1985) firstly demonstrated that proallergic activity of extracellular histones inducing mast cell degranulation (histamine release)[51].

Recent study reported by Nakano, *et al.,* the pathogenicity of histone H1 in sepsis and transplantation-induced immune rejection was clarified[52,53]. Those diseases include mast cell-related acute responses. In sepsis, mast cells activated *via* TLR-4 inhibit phagocyte activity and aggravate survival rate in mice. In graft rejection, mast cells interacted with Treg secrete IL-9 which enhance immune tolerance[54,55]. Because thus pathophysiological relationship between histone H1 and mast cell-related acute responses were suggested, I tried to elucidate the proallergic roles of endogenous histone H1, and its *in vivo* kinetics in allergic disorders with using allergic-rhinitis model mice and both *in vitro* and *in vivo* type I allergic reaction model assays.

2. Materials and methods

2.1. Mice and ethical statements

Lewis rats (male, five-week-old) and BALB/c mice (female, 5 weeks old) were purchased from the National Laboratory Animal Breeding and Research Center (Taipei, Taiwan) or Charles River Laboratories (Yokohama, Japan), and were fed with commercial diet and sterile distilled water *ad libitum* under specific pathogens-free condition at 23 ± 3°C with 12 hrs light-dark cycles. All serum samples were stored at -80°C until analysis.

The following experimental design was reviewed and approved by the Institutional Animal Care and Use Committee in Kaohsiung Chang Gung Memorial Hospital or the Committee on Animal Experimentation of Hiroshima University.

2.2. Ovalbumin (OVA)-specific allergic rhinitis model mice

OVA-specific allergic rhinitis model mice were prepared by previously described protocols with some modification[56,57]. BALB/c mice (n = 14) were immunized by intraperitoneal injection with a mixture of 20 μg OVA (Sigma, St. Louis, MO, USA) and 2 mg adjuvant alum (Thermo Fisher Scientific Inc., Rockford, IL, USA) dissolved in 100 μl PBS, twice with 2 weeks interval. After 2 weeks, their allergic rhinitis-like nasal symptoms were induced by daily nasal challenge with OVA (positive control: 0.4 μg/20 μl/mouse, n = 4) for 6 days, with using PBS (negative control: 20 μl/mouse, n = 4) as a

negative control. To evaluate the proinflammatory role of histone H1 in allergic rhinitis, instead of OVA, calf thymus linker histone H1 (0.4 μg/20 μl/mouse, n = 4, Merck Millipore, Billerica, MA, USA) was used for nasal challenge. As sham control mice (n = 6) were intraperitoneally immunized with PBS/alum instead of OVA/alum, and their nasal challenge were performed with calf thymus histone H1 (0.4 μg/20 μl/mouse, n = 3) or PBS (negative control: 20 μl/mouse, n = 3). To evaluate the nasal symptoms, their sneezing were counted for 5 min after daily nasal challenge.

2.3. Quantification of circulating histone H1 in serum

The serum levels of histone H1 before and after intraperitoneal immunization with OVA/alum were measured by enzyme-linked immunosorbent assay (ELISA), following previously described protocol[58,59]. An anti-histone H1 polyclonal Ab (0.1 μg, Santa Cruz Biotechnology, Santa Cruz, CA, USA) dissolved in 50 μl bicarbonate buffer (100 mM $NaHCO_3$, pH 9.3) was coated on a 96-well microtiter plate (Nalge Nunc International, Roskilde, Denmark) at 4°C, overnight. After three times washing with washing buffer (0.05% tween 20 dissolved in PBS, pH 7.2), the plate was blocked with 300 μl blocking buffer (2% bovine serum albumin (BSA) dissolved in PBS containing 0.05% tween 20) at 4°C, for 60 min. After three times washing, serum samples (50 μl, 25-fold diluted with dilution buffer (0.9% NaCl, 10 mM Tris-HCl, pH 8.0, and added with 0.05% Tween 20) were

applied to the plate with using calf thymus histone H1 (50 μl; 0, 0.31. 0.63, 1.25, 2.5, 5, 10 and 20 μg/ml) as a standard, at room temperature, for 1 hr. After three times washing, 50 μl detecting Ab (anti-histone H1 monoclonal Ab, 500-fold dilution with dilution buffer, Abcam, Cambridge, MA, USA) was then applied and the plate was incubated for 1 hr at room temperature. After three times washing, 2nd Ab (peroxidase-conjugated anti-mouse IgG, 2,000-fold dilution with dilution buffer, Santa Cruz Biotechnology) was then applied and the plate was incubated for 1 hr at room temperature. After five times washing, the plate was colored by 1-Step Ultra TMB substrate solution (100 μl, Thermo Fisher Scientific Inc.) and stop solution (100 μl, 2N HCl). Its absorbance (450 nm) was measured by using a Victor X4 Multilabel Plate Reader (PerkinElmer, Shelton, CT, USA).

2.4. Enzyme-linked immunosorbent assay (ELISA) for total and OVA-specific immunoglobulins

The serum levels of total IgE and OVA-specific IgG1, IgG2a and IgE were quantified by ELISA as described previously[57]. The antibodies for ELISA were purchased from BD Biosciences (San Jose, CA, USA). In total IgE quantification, coating Ab (anti-mouse IgE Ab, 250-fold dilutied with 100 mM $NaHCO_3$, 500 mM NaCl, pH 8.5) was coated at 4°C, overnight. After three times washing with washing buffer, the plate was blocking with 300 μl blocking buffer (1% BSA in PBS) at 37°C, for 2 hrs. After three times

washing, 50 μl serum 10-fold diluted with blocking buffer were applied and the plate was incubated at 37°C, for 2 hrs. After three times washing, detecting Ab (biotin conjugated anti-mouse IgE Ab, 250-fold diluted with blocking buffer) was added and the plate was incubated at 37°C, for 90 min. After three times washing, 200-fold diluted streptavidin-horseradish peroxidase (HRP, R&D Systems, Minneapolis, MN, USA) was added and the plate was incubated at 37°C, for 1 hr. After five times washing, the plate was colored by TMB substrate solution (100 μl) and 2N HCl (100 μl). Its absorbance at 450 nm was measured by using a Victor X4 Multilabel Plate Reader.

To determine the level of OVA-specific immunoglobulins, 2.5 μg OVA dissolved in PBS was coated on 96-well microplates at 4°C, for overnight. After three times washing, the plate was blocked with 1% BSA dissolved in PBS at 37°C, for 2 hrs. After three times washing, serum samples (IgG1: 10,000-fold dilution, IgG2a: 1,000-fold dilution, IgE: 10-fold dilution with blocking buffer) were applied and the plate was incubated at 37°C, for 2 hrs. After three times washing, detecting Ab (biotin-conjugated anti-mouse IgG1, IgG2a or IgE Ab 250-fold diluted) was added and the plate was incubated at 37°C, for 90 min. After three times washing, streptavidin-HRP (200-fold dilution) was added and the plate was incubated at 37°C, for 1 hr. After five times washing, the plate was colored by 1-Step Ultra TMB substrate solution and 2N HCl. Its absorbance at 450 nm was measured by using a Victor X4 Multilabel Plate Reader.

2.5. Histological analysis of nasal mucosal tissues

The specimens were prepared from OVA-specific rhinitis model mice after the final nasal challenge, and their heads were kept in 10% formaldehyde. Histological analysis of nasal mucosal tissues was consigned to Litzung Biotechnology Inc., (Kaohsiung, Taiwan) following the previous report[60]. Briefly, the specimen's skin, eyes and lower jaw was removed, and the skull was sectioned posterior. The head was decalcified and fixed by immersing in a commercial decalcification buffer (Leica Microsystems Canada, Inc., Manitoba, Canada). The specimen was washed in 70% ethanol, subsequently dehydrated in ethanol series (finally in 100% ethanol). Then completely dried specimen was immersed in xylene, subsequently in paraffin: xylene=1:1 solution, finally in paraffin. It was putted in embedded pack, and then solidified in cold water. The sectioned nasal mucosa (4 μm) was deparaffinized with remosol, and washed with 100% ethanol and 70% ethanol. The section was stained with hematoxylin and eosin (H&E) or toluidine blue to assess inflammatory cell infiltration. After washing with water and dehydrated, eosinophils and mast cells were counted under a microscope at 400-fold magnification. At least six randomly chosen high power fields (HPFs) of each section were examined to yield the mean number of eosinophils or mast cells per HPF in the nasal septal mucosa.

2.6. Mast cell degranulation and proinflammatory cytokines production

To evaluate the impact of histone H1 in allergic reactions, calf thymus histone H1 (Merck Millipore) was applied to mast cell. Mast cell model, rat basophilic leukemia cell line (RBL-2H3), was purchased from Cell Bank of RIKEN BioResource Center (Ibaraki, Japan). RBL-2H3 shows typical characteristics of both mucosal mast cell and basophil[61]. RBL-2H3 cells were maintained in Modified Eagle Medium (MEM) containing 10% fetal bovine serum, 100 U/ml penicillin and 100 μg/ml streptomycin with 5% CO_2 at 37°C. Dead cells were removed by washing with PBS during maintenance, while viable cells were collected with using trypsin-EDTA and centrifugation at 190 x *g*, for 5 min. In mast cell degranulation assay, RBL-2H3 cells at log phase were seeded to a 96-well flat bottom plate as 6 x 10^4 cells/well (200 μl) and incubated for 8 hrs, and sensitized with 10 ng/well anti-2,4-Dinitrophenyl (DNP) IgE for 16 hrs. After washing with modified Tyrode's buffer (MT buffer: 20 mM HEPES, 135 mM NaCl, 5 mM KCl, 1.8 mM $CaCl_2$, 1 mM $MgCl_2$, 5.6 mM D(+)-glucose, and 0.05% BSA; pH7.2), they were incubated in the presence of calf thymus histone H1 dissolved in MT buffer at 37°C, for 30 min. To evaluate augment effect of histone H1 on mast cell degranulation induced by DNP-BSA, RBL-2H3 (2×10^5 cells/ml) were sensitized with anti-DNP IgE, and they were incubated with histone H1 (25, 50 and 100 μg/ml) for 30 min following by incubation with DNP-BSA (1.0 μg/ml, Invitrogen) for 30 min. The supernatants were collected, and 0.5% Triton X-100 dissolved in Tyrode's buffer was added for quantification total

granules in the cells. To evaluate the degranulation rate, β-hexosaminidase activity included in granules of sample supernatant was measured as an index of degranulation. Substrate solution (20 μl, 1.3 mg/ml *p*-nitrophenyl-N-acetyl-β-D-glucosaminide dissolved in 4 mM sodium citrate buffer, pH 4.5) was mixed with 30 μl samples and incubated at 37°C, for 1 hr. The enzymatic reaction was stopped by 150 μl of stop buffer (0.2 M glycine, pH 10.0). Its absorbance at 405 nm was measured by using a Victor X4 Multilabel Plate Reader. The percentage of degranulation was calculated by the following formula: Degranulation rate (%) = 100 × absorbance of supernatant/(absorbance of supernatant + absorbance of cell lysate). To evaluate the proinflammatory cytokine (IL-6 and TNF-α) productions, sample supernatants were applied to Rat IL-6 and TNF-α ABTS ELISA Development Kits (PeproTech, NJ, USA) with following to the manufacturer's protocols.

2.7. Western blot analysis for extracellular histone H1 secreted by mast cells

To determine whether mast cell could secrete histone H1 themselves, Lewis rat bone marrow-derived mast cells (BMMCs) were prepared following the previous study[62]. Bone marrow was collected from femur, and the cells were sufficiently suspended and seeded in Roswell Park Memorial Institute medium (RPMI 1640, Invitrogen) containing with 4 ng/ml mouse recombinant IL-3 (Sigma), 1 mM sodium pyruvate (Wako Pure Chemical Industries, Ltd., Osaka, Japan), 1 mM MEM Non-essential Amino Acids

Solution (Wako), 50 μM 2-mercaptoethanol (Nacali tesque, Kyoto, Japan), and 1 mM HEPES (Thermo). The cells were maintained at 37°C, 5% CO_2, for 3 weeks. After harvesting of the cells by centrifugation at 250 x *g*, for 5 mins, the BMMCs (1 x 10^6 cells/ml) were seeded and sensitized with anti-DNP IgE (0.5 μg/ml, Sigma) for 18 hrs, at 37°C. After washing with MT buffer, they were incubated in the presence of DNP-BSA for 1 hr, at 37°C. The supernatants (5 μl) and calf thymus histone H1 (10 μg) were mixed 1:1 ratio with two-fold-concentrated sample buffer (0.1 M Tris-HCl, 4% SDS, 20% glycerol, 10% 2-mercaptoethanol, 1% bromophenol blue, pH6.8), and incubated at 100°C for 8 min. Those samples were applied electrophoresis in a 12.5% SDS-PAGE gel (mini gel apparatus,Bio-Rad, Burlington, MA, USA), and the proteins were electronically transferred onto a PVDF membrane (GE Healthcare Bio-Sciences Corp.). The membrane was blocked with 5% non-fatty skim milk dissolved in TBST (50 mM Tris hydroxymethyl aminomethane, 150 mM NaCl, and 0.1% tween-20, pH7.5) for 1 hr, at room temperature. After washing with TBST for 5 min, twice, the membrane was immunoprobed with rabbit polyclonal Ab against histone H1 (200-fold dilution with 5% skim milk/TBST, Santa Cruz Biotechnology) at 4°C, overnight, subsequently incubated with peroxidase-conjugated goat anti-rabbit IgG (10,000-fold dilution; Santa Cruz Biotechnology) at room temperature, for 2 hrs. Its signals were detected by using an ECL Plus Western Blotting Detection System (GE Healthcare Bio-Sciences Corp.).

2.8. Passive cutaneous anaphylaxis (PCA) model mice

Passive cutaneous anaphylaxis (PCA) reaction in ear was performed as previous protocol with some modification[63]. An anti-DNP IgE (150 ng/10 μl, Sigma) mixed with calf thymus histone H1 (10 μg) was intradermally injected in the right ear. As a blank, PBS mixed with histone H1 (10 μg) was intradermally injected in the left ear (n = 3). As a control (n = 3), anti-DNP IgE and PBS were injected without histone H1, respectively. After 24 hrs, 200 μg of DNP-human serum albumin (HAS, Sigma) dissolved in 100 μl of Evans blue solution (0.5%, Tokyo Chemical Industry, Co., Ltd., Tokyo, Japan) was intravenously injected to induce anaphylaxis. After 30 min, those mice were sacrificed by cervical dislocation. Their PCA responses were evaluated by amount of exudate Evans blue dye in the ears. The dye was extracted by overnight incubation with formamide at 63°C, and its absorbance (595 nm) was measured by using a Wallac 1420 ARVOsx Multilabel Counter (Perkin-Elmer).

2.9. Statistical analysis

Each data was composed of triplicate sample and contained standard deviation expressed as mean ± S.D. Non-paired two-tailed Student's t-test was used to assess statistical significance of difference compared to corresponding controls. Statistical significance was defined as $p < 0.05$.

3. Results

3.1. Elevation of serum levels of histone H1 upon immunization with OVA

To explore the relationship between histone H1 and allergic immunization *in vivo*, serum histone H1 levels before and after immunization by intraperitoneal injection with OVA/adjuvant alum were compared (Fig. 4A). As shown in Fig. 4B, histone H1 expressed significantly higher level after immunization with OVA/alum, but not with PBS/alum. I confirmed that OVA-specific IgE levels were increased by OVA/alum immunization, but not by PBS/alum (Fig. 4C). Thus elevation of serum histone H1 levels showed correlative trend with construction of allergic condition with up-regulation of antigen-specific IgE.

3.2. Histone H1 challenge induced nasal symptoms even without OVA sensitization in OVA-immunized mice

To explore the pathophysiological role of histone H1 in the model of allergic rhinitis, histone H1 was intranasally challenged to OVA-immunized mice (Fig. 5A). As shown in Fig. 5B, nasal challenge of histone H1 even without OVA dramatically developed nasal symptoms of allergic rhinitis in OVA-intraperitoneally immunized mice, as compared with those of naive mice (PBS/alum-immunized and PBS-nasally challenged). Additionally, histone H1-induced sneezing was significantly severer than OVA-induced sneezing in OVA-immunized mice. Interestingly, histone H1 challenge failed

to develop nasal symptoms in PBS-immunized mice, suggesting that proallergic potency of histone H1 is related to OVA-specific IgE-dependent reaction such as mast cell degranulation for developing allergic symptoms. The histological analysis showed that histone H1 challenge enhanced infiltration of eosinophils and mast cells into the lesion of intranasal mucosal tissues in OVA/alum immunized mice (Fig. 5C and D).

3.3. Enhancement of IgE-mediated degranulation from mast cells by histone H1

To evaluate the pathophysiological effect of histone H1 on mast cell-mediated allergic reactions *in vitro*, histone H1 was exogenously applied into *in vitro* degranulation assay by using RBL-2H3 cells. As shown in Fig. 6A, histone H1 induced IgE-sensitized mast cell degranulation even without antigen (Ag; DNP-BSA), and proinflammatory IL-6 and TNF-α production (Fig. 6B). Moreover, histone H1 potentiated Ag-induced degranulation in a dose-dependent manner (Fig. 6C). Because mast cells secrete nucleosome during infection[64], I next tried to confirm whether mast cells secrete histone H1 in type I allergic responces. The supernatant of reaction buffer after Ag-induced degranulation was applied to SDS-PAGE and western blot analyses with anti-histone H1 Ab. As shown in Fig. 6D, the extracellular histone H1 was detected around the molecular weight of 60 kDa, while purified histone H1 was detected in 60 kDa and 34/31 kDa, suggesting that the secreted histone H1 formed a dimer as described in a previous report[65].

This hypothesis was demonstrated by Electrospray ionization (ESI)-MS/MS analysis of the 60 kDa band whose internal amino acid sequences and coincided with that of histone H1 (Table 1). Taken together, histone H1 acts factor on IgE-dependent mast cell degranulation.

3.4. Exacerbation of allergic inflammation by histone H1 in mast cell-driven PCA model mice

To evaluate the *in vivo* augmentation effect of histone H1 on IgE-mediated mast cell reactions, exogenous histone H1 was auricle-intradermally injected to mast cell-driven PCA model mice after auricle anti-DNP IgE-intradermal sensitization and DNP-HSA-intravenous injection (Fig. 7A). The PCA level was evaluated by level of Evans blue exuded in ears. As shown in Fig. 7B and C, histone H1 significantly exacerbated PCA response in the presence of IgE, while histone H1 failed to enhance the reaction in the absence of anti-DNP IgE, as compared with each controls (right ear driven by IgE-sensitized PCA and left ear driven by PBS-sensitized PCA). These results demonstrated that histone H1 enhanced IgE-mast cell-axis-driven allergic inflammation even when *in vivo* conditions.

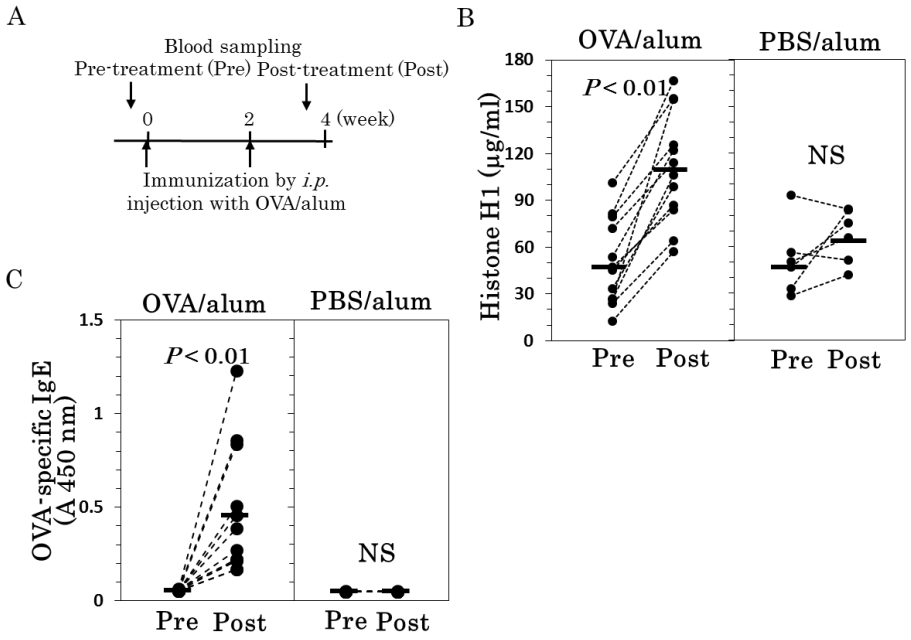

Fig. 4. Elevation of serum histone H1 levels by OVA/alum immunization and its correlation with OVA-specific IgE production. (A) A scheme of blood samplings of mice twice intraperitoneally (*i.p.*) immunized with OVA/alum. The level of histone H1 (B) or OVA-specific IgE (C). Each two symbol connected by dashed line means individuals of those mice and its bar indicates mean value. NS: not significant.

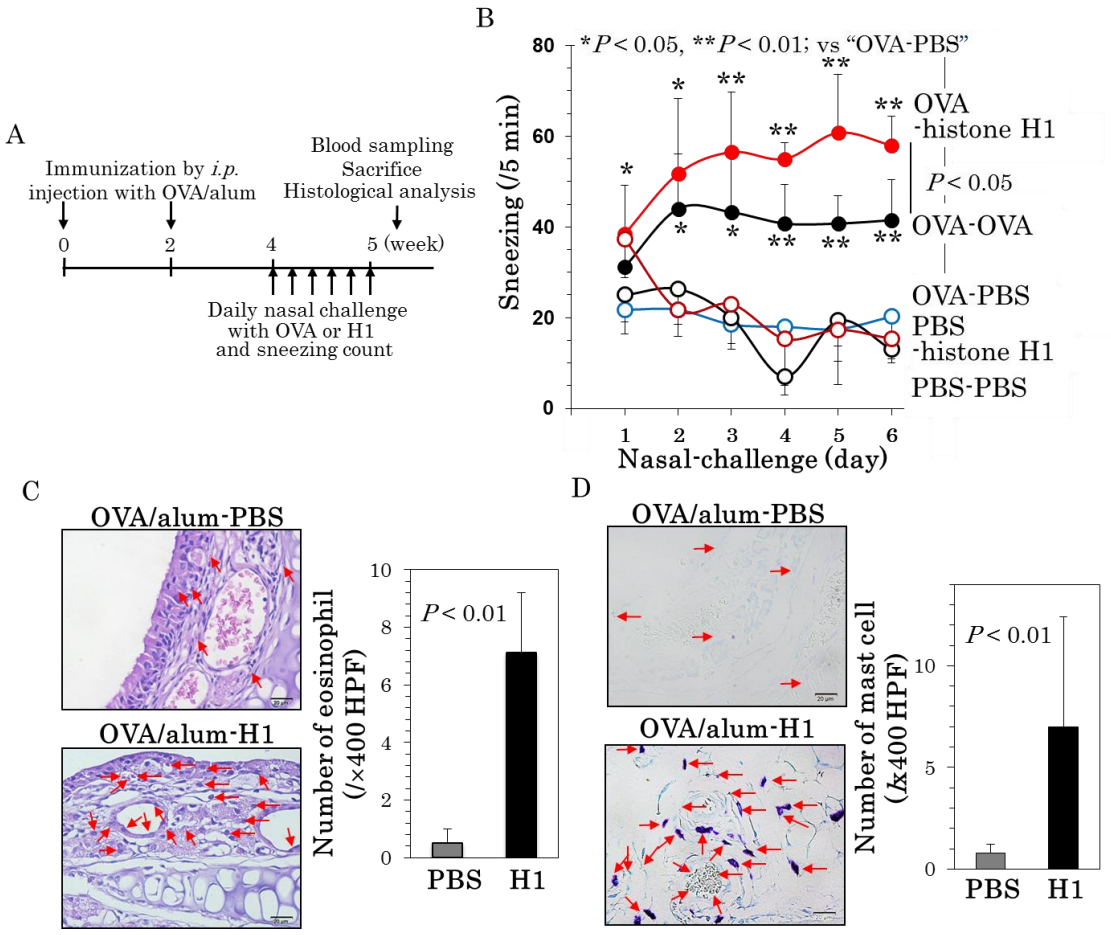

Fig. 5. Development of allergic rhinitis-like nasal symptoms by histone H1-challenge in OVA-immunized mice. (A) A scheme of evaluating impact of nasal challenge with histone H1 in OVA-immunized mice. (B) Time course of nasal symptoms was evaluated by sneezing count for 5 min after daily nasal challenge (In OVA *i.p.*-immunized mice, histone H1 (OVA-histone H1), OVA (OVA-OVA) or PBS (OVA-PBS) were nasally challenged respectively. In PBS *i.p.*-immunized mice, histone H1 (PBS-histone H1) or PBS (PBS-PBS) were nasally challenged respectively.). (C and D) Representative sections of the intranasal mucosal tissue in OVA-PBS (upper figures) or OVA-histone H1 (downer figures). Eosinophils stained by H&E (C) and mast cells stained by toluidine blue (D) were shown by red arrows. Values are presented as the mean ± S.D.

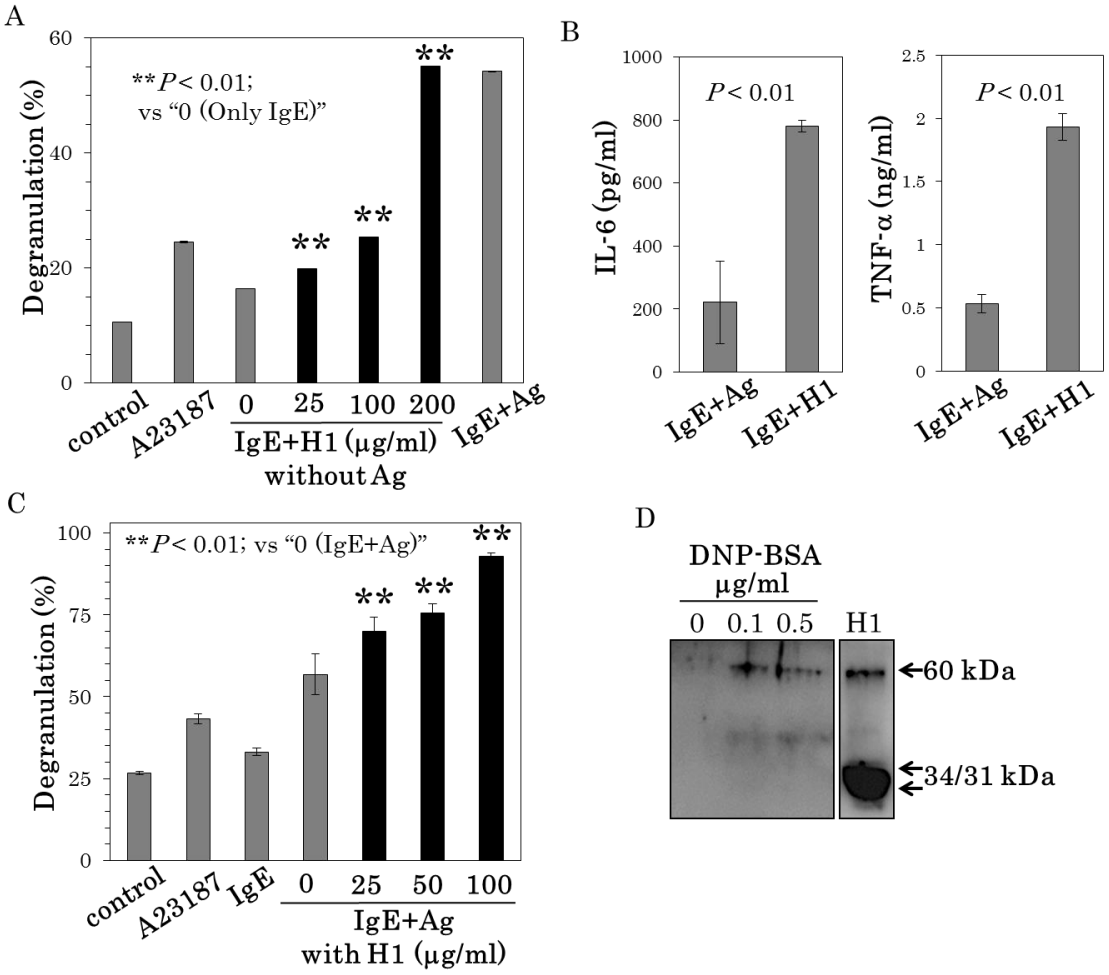

Fig. 6. Enhancement of mast cell-reaction by histone H1 under IgE-sensitized condition. (A, C) Calcium ionophore A23187 (10 μM) is as a positive control for degranulation. Data shows the mean ± S.D. (A) Histone H1 induced degranulation from IgE-sensitized RBL-2H3 even without DNP-BSA in a dose dependent manner. (B) Histone H1 (100 μg/ml) also up-regulated proinflammatory IL-6 and TNF-α production without DNP-BSA. (C) Histone H1 also enhanced Ag-induced degranulation in a dose-dependent manner. (D) Representative result of western blot analysis using histone H1-specific antibody against supernatant of reaction buffer after DNP-BSA-induced degranulation from IgE-sensitized rat BMMCs, and control histone H1.

Table 1. ESI-MS/MS analysis of 60 kDa antigen secreted in the supernatant of mast cells reaction buffer[a]

	Protein description[b]	MOWSE score[c]	Experimental Mr / pI[d]	Theoretical Mr / pI[e]
Histone H1	Histone (H1d)	1130	60.00 / N.A.	21.83 / 11.10
	Histone H1.2	1065		21.30 / 11.01
	Histone H1.5	600		22.64 / 10.97
	Histone H1.1	398		21.99 / 10.99

.

[a]The 60 kDa band of supernatans of reaction buffer after DNP-BSA-induced degranulation from IgE-sensitized mast cell as shown in Fig. 6D was applied to liquid chromatography-ESI-MS/MS analysis by Visual Protein Biotech Corp. (Taipei, Taiwan).

[b]Candidate proteins.

[c]MOWSE (Molecular Weight SEarch) method identify proteins from the molecular weight of its peptides created by proteolytic digestion on MS/MS. Score = -10log$P$

[d,e]Mass-to-charge ratio (Mr), isoelectric point (pI), not applicapable (N.A.)

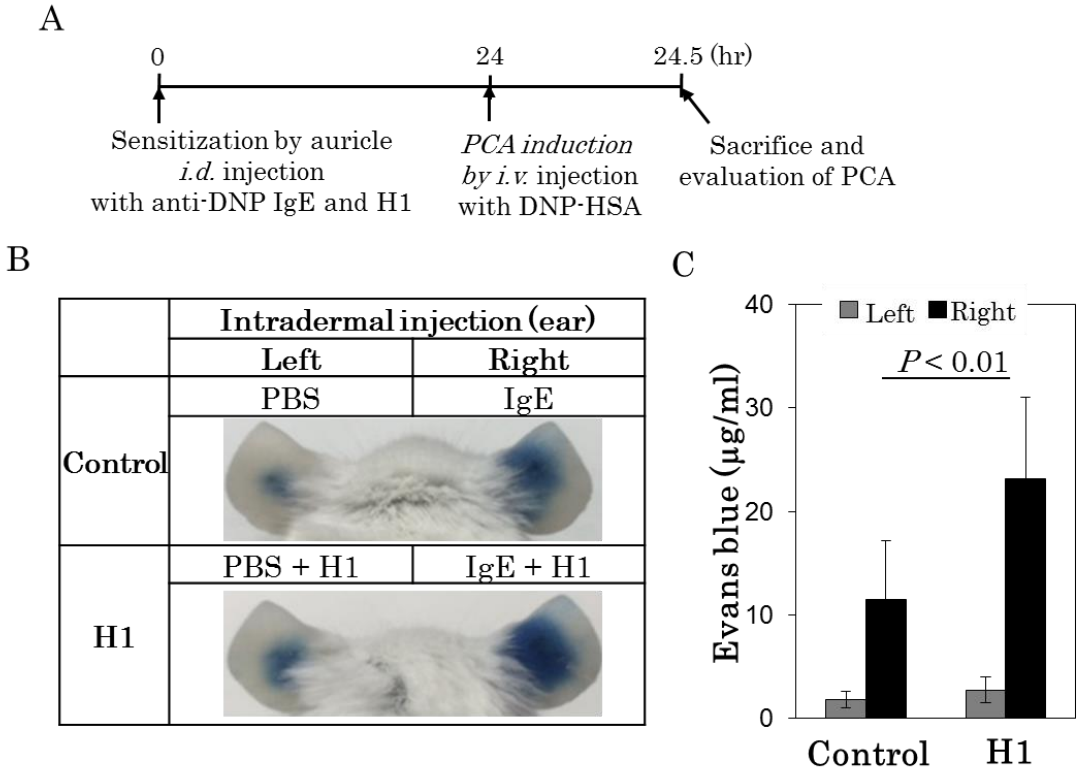

Fig. 7. Exacerbation of IgE-mediated PCA reaction by histone H1. (A) A scheme of PCA reaction in mice. (B) The pictures are representatives of individuals in each group. (C) The level of Evans blue dye extracted from their ears was evaluated by absorbance of 595 nm. Each data indicates mean values including S.D.

4. Discussion

The proallergic role of nuclear antigens mostly remains unclear. The present study shows the remarkable impact of endogenous extracellular histone H1 on the progression of type I allergic responses in allergic rhinitis model mice as well as mast cell degranulation.

As shown in Fig. 4, elevation of serum histone H1 level showed a good correlation with increasing antigen-specific IgE titer. Taken together with previous report describing induction of LPS-stimulated DC maturation by extracellular histone H1[66], histone H1 possibly exerts Th2 responses. Nasal challenge with exogenous histone H1 dramatically progressed allergic rhinitis-like symptoms as well as expansion of mast cells in nasal mucosa even without antigen in antigen-immunized mice (Fig. 5). The *in vivo* results corresponded to the *in vitro* results showing that histone H1 induced mast cell degranulation and proinflammatory IL-6 and TNF-α production even without antigen in the presence of IgE (Fig. 6A and B). Histone H1 also enhances mast cell expansion *via* IL-6 up-regulation by protecting mast cell from IL-4 induced apoptosis[67], which may be related with mast cell expansion in nasal mucosa (Fig. 5D). Moreover, histone H1 augmented antigen-induced mast cell degranulation both in *in vitro* degranulation assay (Fig. 6C) and *in vivo* PCA analysis (Fig. 7). Induction of degranulation from IgE-sensitized mast cells even without antigen was demonstrated by using protein Fv (the protein is an endogenous protein produced in liver)

with its IgE-superantigen activity[68]. Those data suggested that extracellular histone H1 may act as endogenous "IgE-superantigen". My data indicated that histone H1-driven degranulation requires a presence of IgE, although previous reports indicated that histone H1 induced degranulation from plane mast cells[51,69]. Only difference of experimental conditions is that I used mucosal type RBL-2H3, while they used rat peritoneal mast cell of tissue-connecting type. These are several differences among their phenotypes, especially, in expression levels of Mas-related G-protein coupled receptors (Mrg receptors) which recognizes potently positive charge compounds to induce degranulation. It is lower in mucosal type mast cell than in tissue-connecting type[23,70]. Considering that histone H1 includes base-rich amino acid residues such as lysine and arginine, histone H1 may be also recognized by Mrg receptor. Therefore, it is necessary to elucidate the effect mechanism on degranulation signal transduction. Interestingly, secreted histone H1 was detected in mast cell medium after antigen-induced degranulation (Fig. 6D), suggesting autocrine activity of histone H1 upon mast cell activation (Fig. 8).

Taken together, endogenous histone H1 released from wound or by stress at the antigen-invasion phase contributes to onset of the antigen-specific immune responses, and the severe allergic symptoms at the pathogenesis phase escalates. Thus proallergic activity of extracellular histone H1 is very important in allergic disorders so as to have potential of therapeutic target.

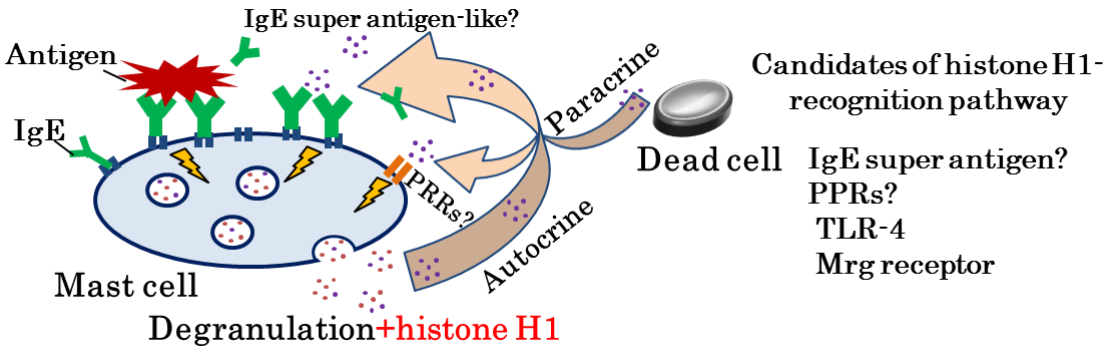

Fig. 8. Overview of histone H1 kinetics on mast cell activation

Chapter 2:

Therapeutic potential of histone H1-neutralizing antibody against type I allergic disorders

1. Introduction

In chapter 1, I found that histone H1 acts as a proallergic factor enhancing IgE-mast cell axis reaction. Therefore, disturbance of this histone H1-mediated innate immune responses would be a therapeutic target for type I allergic diseases. Anti-histone H1 antibody has been showed anti-inflammatory activity in experimental sepsis-like syndrome in which plasma and lung proinflammatory cytokines including IL-1β, IL-6 and TNF-α has been downregulated[52]. The immunosuppressive effect of anti-histone H1 antibody was also demonstrated in liver transplantation[71].

The present chapter shows anti-allergic activity of histone H1-targeted antibody with disturbance of the autocrine degranulation activity of histone H1.

2. Materials and methods

2.1. Ethical statements

The following experimental design was reviewed and approved respectively by the Institutional Animal Care and Use Committee in Kaohsiung Chang Gung Memorial Hospital or the Committee on Animal Experimentation of Hiroshima University.

2.2. Mice and immunosuppressive monoclonal antibody against histone H1 peptide mimotope (anti-histone H1 mAb; SSV mAb)

BALB/c mice (female, five-week-old) were purchased form the National Laboratory Animal Breeding and Research Center or Charles River Laboratories. They were bred with sterile distilled water and commercial diets *ad libitum* under specific pathogens-free condition at 23 ± 3°C with 12 hrs light-dark cycles. All serum samples were stored at -80°C until analysis. The anti-histone H1 mAb (SSV mAb, isotype IgG1) corresponding with histone H1 peptide mimotope (SSVLYGGPPSAA) shows inhibitory activity of systematic immune reaction of T cells induced by CD3/CD28 stimulation. I obtained the antibody from Josai International University, Japan [72,73].

2.3. Mast cell degranulation

In vitro IgE-mediated degranulation from RBL-2H3 was performed by previously described in chapter 1. 2.6. RBL-2H3 cells (6 x 10^4 cells/well, 200 μl) were seeded to a 96-well flat bottom plate, and incubated for 8 hrs. They were sensitized with 10 ng/ml anti-DNP IgE, and incubated for 16 hrs, at 37°C. After washing with MT buffer, they were incubated in the presence of SSV mAb or isotype IgG1 control (BD Biosciences) for 30 min. IgE-mediated degranulation was induced by 1.0 μg/ml of DNP-BSA, it was evaluated by measurement of β-hexosaminidase activity in the supernatants. The total granules in the cell were collected with using cell lysis buffer (0.5% triton X-100 in MT buffer).

2.4. PCA model mice

PCA model mice were prepared as protocol previously described in chapter 1. 2.8. Briefly, anti-DNP IgE (150 ng/10 μl) or PBS was intradermally injected in each the right or left ear. As a sham control (n = 8), PBS was intradermally injected in both right and left ears. Twenty-three hrs later, 200 μl of PBS (vehicle control; n = 7), 100 μg of isotype IgG1 (n = 8) or SSV mAb (n = 7) was intravenously injected at their tail vein. After One hr, their anaphylaxis were induced by intravenous injection with 200 μg DNP-HSA dissolved in 100 μl Evans blue solution (0.5%). After 30 min, they were sacrificed and their PCA responses were evaluated by the

measurement of Evans blue dye exuded in the ears. Evans blue dye extracted with formamide overnight was measured by a Wallac 1420 ARVOsx Multilabel Counter with absorbance of 595 nm.

2.5. OVA-specific allergic rhinitis model mice

Immunization and nasal challenge with OVA (Sigma, St. Louis, MO, USA) were performed as protocol previously described in chapter 1. 2.2. BALB/c mice were intraperitoneally immunized twice with adjuvant alumn (2 mg) and OVA (20 μg) dissolved in PBS (100 μl) with two weeks interval. After two weeks from the second immunization, their allergic rhinitis-like nasal symptoms were induced by daily nasal challenge with OVA (0.4 mg/20 μl/mouse) for nine days. To evaluate the therapeutic potential of histone H1-targeted SSV mAb, 100 μg of SSV mAb (n = 4) or isotype IgG1 (n = 5) was intraperitoneally injected before the daily nasal challenge. Their allergic symptoms were evaluated by counting number of sneezing for 5 min after nasal challenge.

2.6. Histological analysis of nasal mucosa

Experimental mice (as 2.5.) were sacrificed after the final nasal challenge, and their heads were kept in 10% formaldehyde solution. Decalcification, dehydration with ethanol, paraffin embedding, sectioning and staining were performed by previously described chapter 1. 2.5.

For immunostaining of local histone H1, section was deparaffined by incubation with lemosol for 30 min, twice. The section was incubated with Peroxidase Block (3% H_2O_2) for 20 min to inactivate endogenous peroxidase, and then incubated in sodium citrate buffer (pH 6.0) at 95°C, for 20 min to activate antigen. The section was washed with following 100% methanol, 100%, 90%, 80%, 70% ethanol and distilled water for 5 min, respectively, and blocked with 5% skim milk for 2 hrs at room temperature. After washing with PBS for 5 min, three times, the section was incubated with rabbit anti-histone H1 polyclonal Ab (100-fold dilution, Santa Cruz Biotechnology) for 2 hrs at 4°C. After washing with PBS for 5 min, three times, the section was incubated with Mouse/Rabbit Probe HRP labeling (BioTnA, Kaohsiung, Taiwan) for 30 min. After washing with PBS for 5 min, three times, histone H1 was visualized by 3,3'-diaminobenzidine staining. Counter staining was carried out using hematoxylin. The section was rinsed with water and covered with resin-based mounting medium (BioTnA) after dehydration with ethanol series.

2.7. Cytokine production in splenocytes

The spleen was harvested from OVA-immunized and SSV mAb treated mice after final OVA nasal challenge described in 2.5., subsequently homogenized and suspended in PBS to remove tissue debris. Then its supernatant was centrifuged at 250 x *g*, for 5 min, and added with

hemolysis buffer (300 mM NH_4Cl, 30 mM $NaHCO_3$, 0.2 mM EDTA-2Na, pH 7.3). After removing the buffer by PBS washing and centrifugation, they (1 x 10^6 cells/well) were seeded to 96 well plate and cultured for 72 hrs, at 37°C, in 10% FBS/RPMI-1640 medium containing penicillin-streptomycin with OVA (200 μg/ml). The supernatants were collected, and the levels of IFN-γ (10-fold diluted sample), IL-4 (10-fold diluted), IL-5 (10-fold diluted), IL-10 (original), IL-13 (original), and IL-17 (10-fold diluted) were measured by using DuoSet ELISA Development Kits (R&D Systems) with the manufacturer's protocols.

2.8. Statistical analysis

Each data was composed of triplicate sample and contained standard deviation expressed as mean ± S.D. Non-paired two-tailed Student's t-test was used to assess statistical significance of difference compared to corresponding controls. Statistical significance was defined as $p < 0.05$.

3. Results

3.1. Inhibitory activity of IgE-mediated degranulation by SSV mAb

To evaluate a therapeutic potential of SSV mAb on IgE-mediated degranulation, SSV mAb was applied to *in vitro* degranulation assay using RBL-2H3 cells. As shown in Fig. 9, DNP-BSA (Ag)-induced degranulation was significantly suppressed by SSV mAb as compared with that by isotype IgG1 (Iso IgG1, 100 μg/ml), suggesting that SSV mAb has a therapeutic potential.

3.2. Suppression of mast cell-driven PCA by SSV mAb

The *in vivo* therapeutic potential of SSV mAb on mast cell-driven allergic inflammation was evaluated in PCA model mice (Fig. 10A). As shown in Fig. 10B and C, SSV mAb significantly decreased extravasation of the Evans blue dye in their ear as compared with those of both vehicle and isotype controls, which confirmed that SSV mAb has a therapeutic effect against mast cell-driven allergic responses such as anaphylaxis.

3.3. Amelioration of allergic rhinitis-like nasal symptom by SSV mAb without significant impact on antigen-specific immune responses

To further evaluate therapeutic effect of SSV mAb on mast cell-driven allergic responses, SSV mAb was intraperitoneally administrated to

OVA-rhinitis model mice upon intraperitoneal immunization and intranasal challenge with OVA (Fig. 11A). As shown in Fig. 11B, SSV mAb significantly ameliorated the sneezing as compared with the isotype control IgG1. After the last nasal challenge later, their nasal tissue specimens were prepared. The histological analyses indicated that SSV mAb significantly decreased infiltration of eosinophils and mast cells into nasal mucosal tissue as compared with isotype control (Fig. 11C and D).

To elucidate the impact of SSV mAb treatment on OVA-specific immune response, titer of OVA-specific immunoglobulins were evaluated by ELISA. OVA-specific IgE, IgG1, and IgG2a titers were unaffected by treatment with SSV mAb (Fig. 12A-C).

To further evaluate the impact of SSV mAb on OVA-specific immune responses, the cytokine profile on OVA-specific splenocyte reactions was analyzed. Splenocytes derived from OVA-immunized and OVA-challenged mice were stimulated with OVA for three days, and collected supernatants were applied to cytokine ELISA. As shown in Fig. 12D-I, SSV mAb didn't affect cytokine productions (IFN-γ, IL-4, IL-5, IL-10, IL-13, and IL-17). Taken together, histone H1-targeted SSV mAb ameliorated allergic rhinitis-like symptoms without affecting antigen-specific immune responses, suggesting that anti-allergic effect of SSV mAb acts directly on mast cell reactions.

To confirm histone H1-neutralizing effect of SSV mAb, serum of OVA-rhinitis model mice after final nasal challenge was applied in histone H1 ELISA. SSV mAb treatment during term of nasal challenge significantly ameliorated allergic-rhinitis like nasal symptoms (Fig. 13A), however it did not downregulate increasing level of serum histone H1. To further explore histone H1-neutralizing effect of SSV mAb, their specimen was immunostained with anti-histone H1 Ab. As shown in Fig. 13B, SSV mAb dramatically decreased local expression of histone H1 as compared with isotype IgG1 treatment.

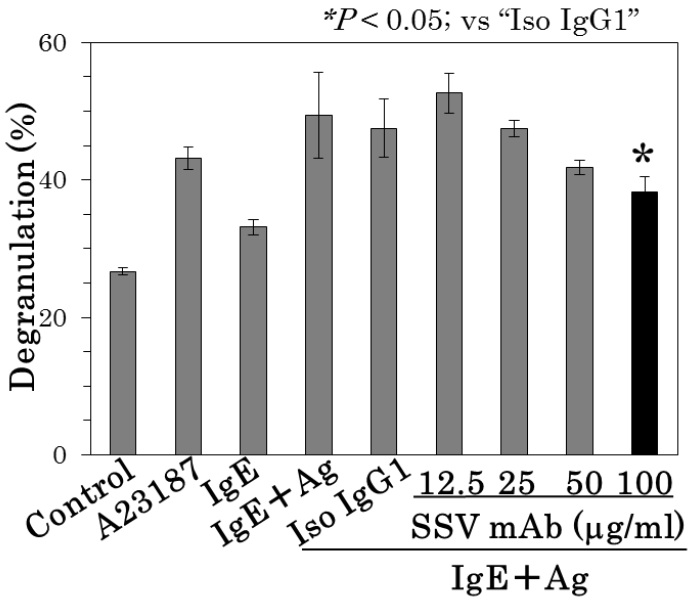

Fig. 9. Inhibition of IgE-crosslinking degranulation from RBL-2H3 by SSV mAb. Concentration of isotype IgG1 (Iso IgG1) was 100 μg/ml. A23187 (10 μM) treated group is as a positive control of degranulation. Each data indicates mean values including ± S.D.

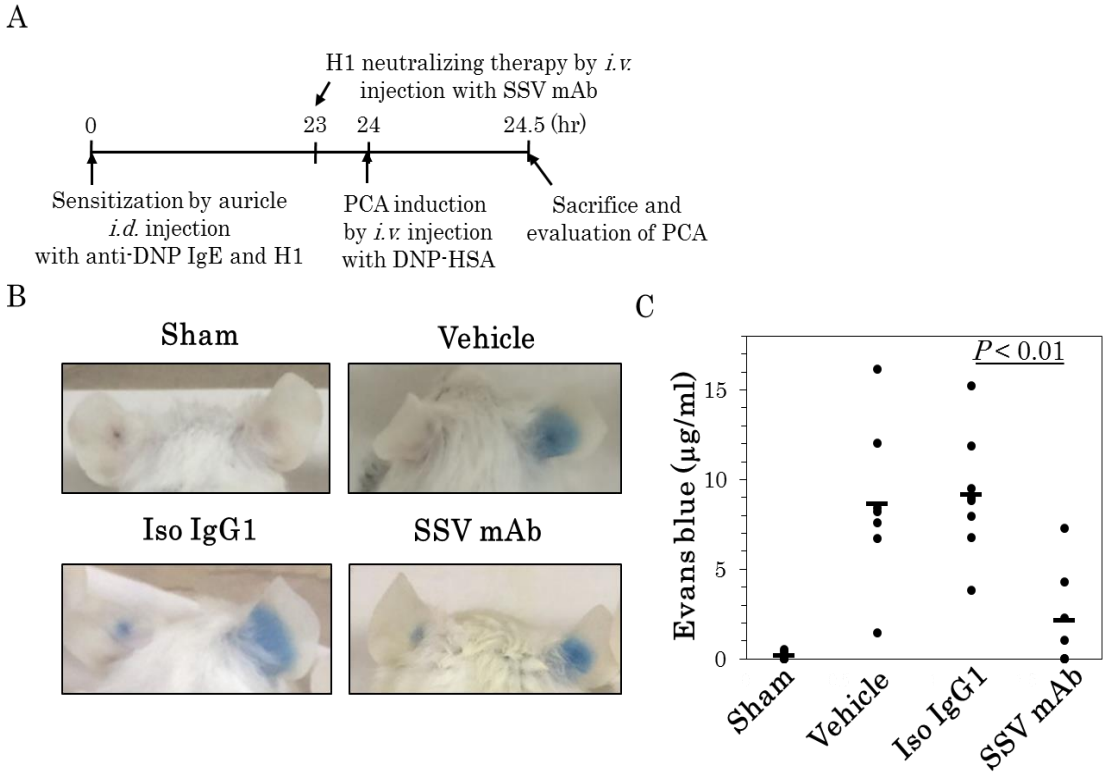

Fig. 10. Inhibition of mast cell-driven PCA reaction by SSV mAb. (A) A scheme of histone H1 neutralization therapy on PCA model mice. (B) The pictures are representative of seven to eight individuals in each group. (C) The level of Evans blue dye extracted from their ears was measured, each whose symbol indicates an individual mouse, and bars show the mean values.

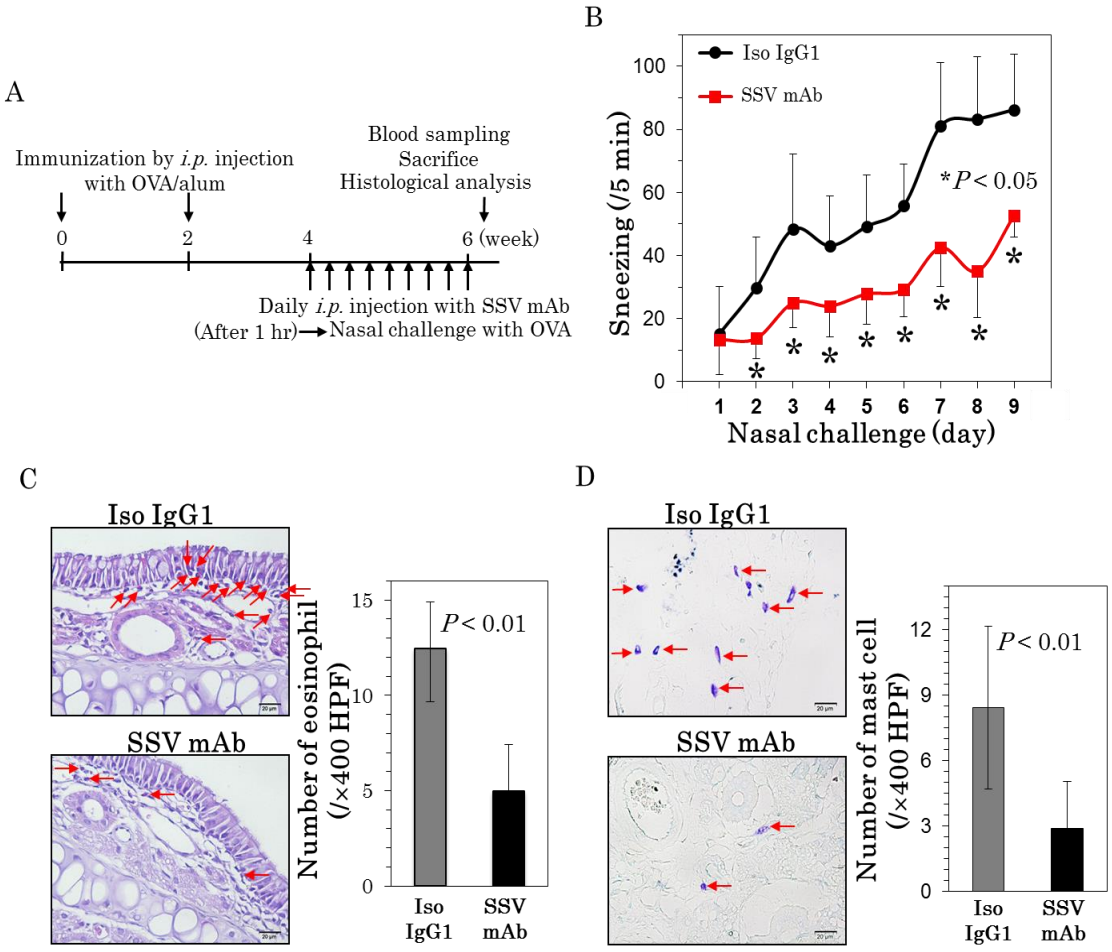

Fig. 11. Therapeutic effect of SSV mAb on allergic rhinitis-like symptoms. (A) A scheme of H1 neutralization therapy on OVA-specific rhinitis model mice. (B) The course of sneezing induced by nasal challenge. Data indicates the mean ± S.D. (C and D) The representative sections of the nasal mucosal tissue of the mice, whose eosinophils (C: H&E staining) and mast cells (D: toluidine blue staining) were shown by red arrows. The count of those cells under a microscope at x400 magnification were shown with the mean ± S.D.

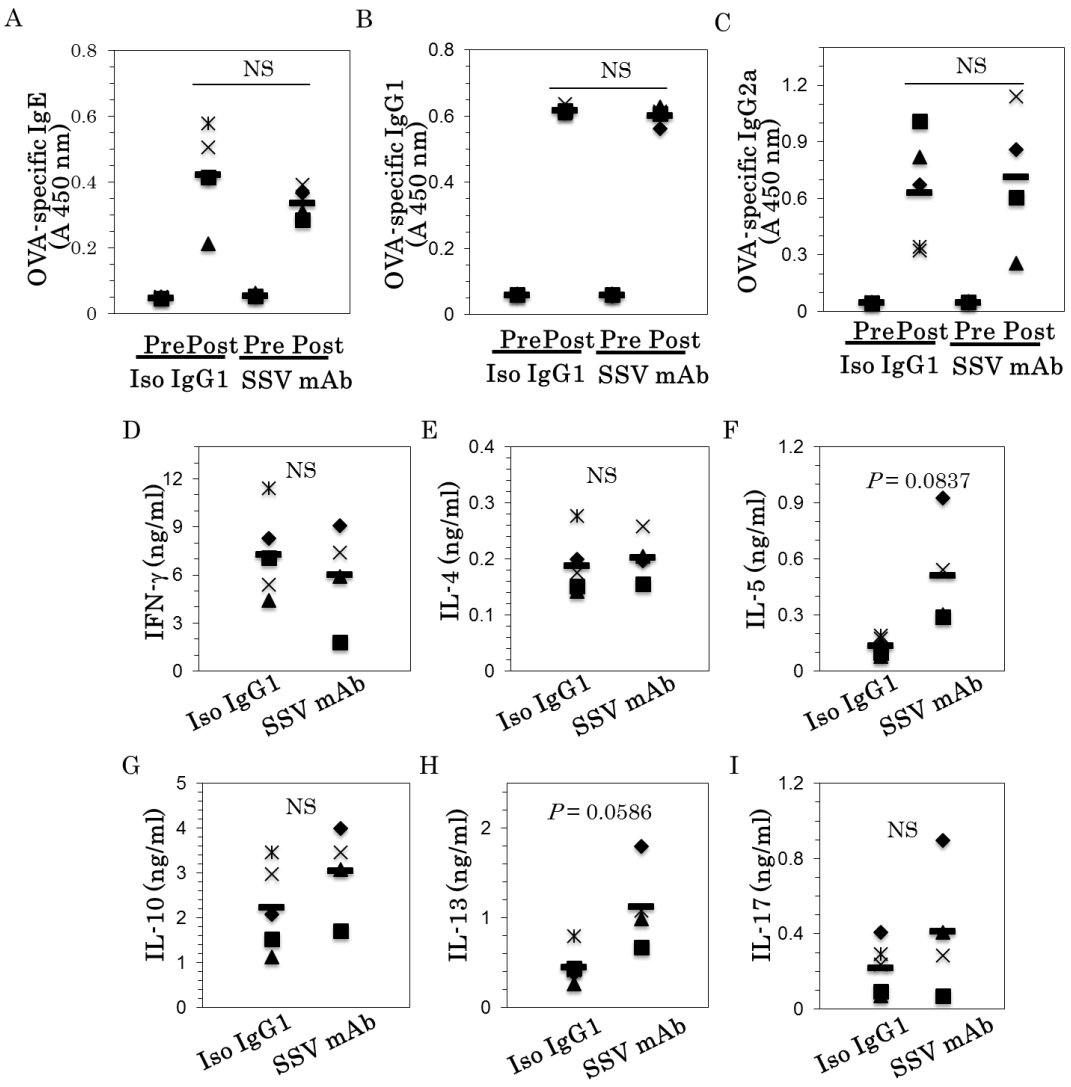

Fig. 12. Serum OVA-specific immunoglobulins titer and cytokine levels released from total splenocytes stimulated with OVA, in OVA-specific allergic rhinitis model mice. (A-C) The serum was collected before immunization (pre) and after final nasal challenge (post, SSV mAb or isotype IgG1), subsequently measured ELISA with OVA-coated plate. Titer of serum OVA-specific IgE (A), IgG1 (B) and IgG2a (C) were shown. (D-I) Cytokine levels (A: IFN-γ, B: IL-4, C: IL-5, D: IL-10, E: IL-13, and F: IL-17) were measured by each ELISA kit. Each symbol indicates an individual mouse, and bars show the mean values. NS: not significant.

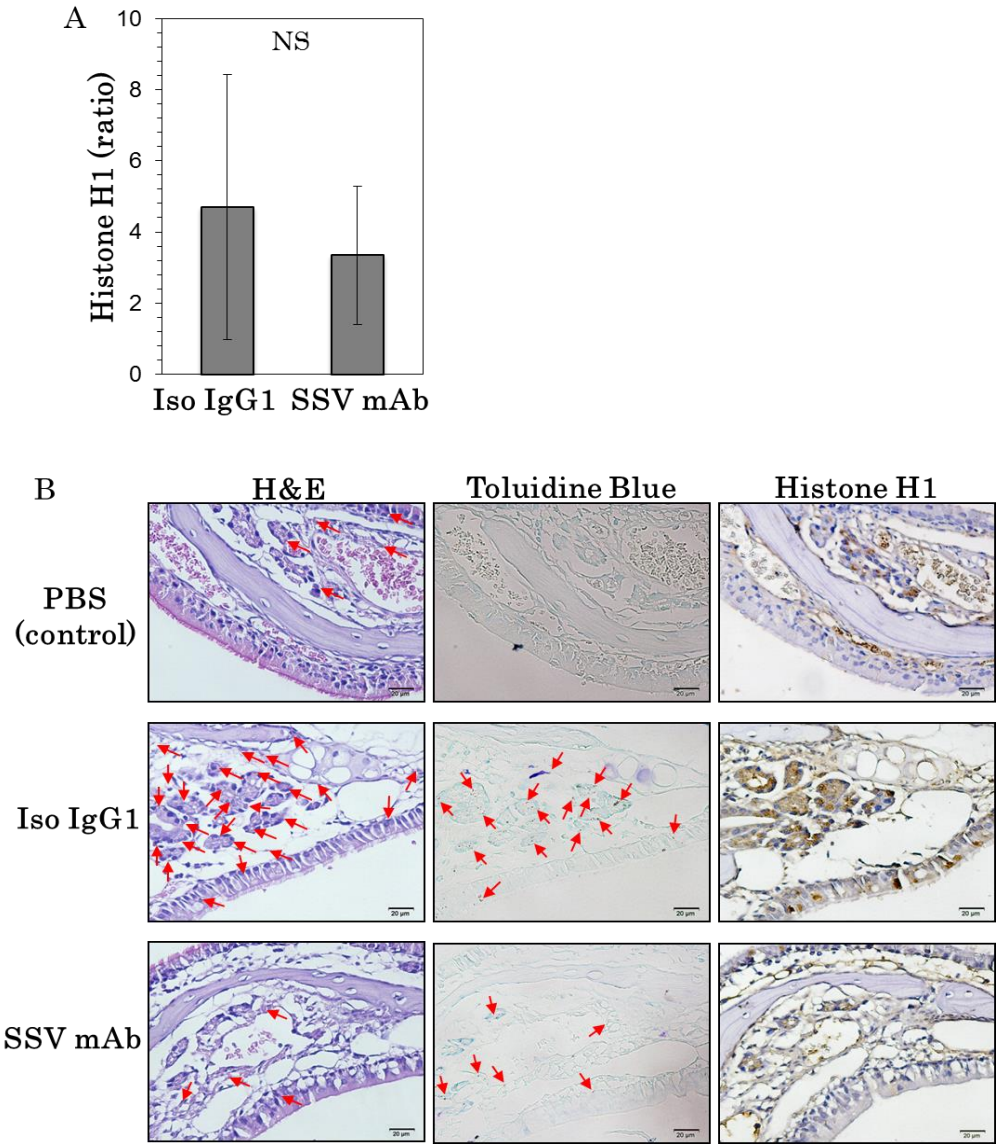

Fig. 13. Impact of SSV mAb for neutralizing serum and local histone H1 in OVA-rhinitis model mice. (A) Ratio of serum histone H1 levels before and after nasal challenge with OVA in OVA-immunized mice was measured by ELISA. Data show mean ± S.D. NS: not significant. (B) Histology staining of nasal mucosal tissues after final nasal challenge. PBS control as a sham control was immunized and nasal challenge with PBS. Eosinophils (H&E staining) and mast cells (toluidine blue staining) indicated red arrows, and histone H1 (immunostaining with anti-histone H1 Ab; shown brown color) were detected in the serial sections (x400 magnification).

4. Discussion

In present chapter, to develop a new strategy for allergy therapy, I focused on endogenous danger signaling molecule which enhance mast cell-mediated allergic responses. Because endogenous histone H1 was demonstrated as a novel auto/paracrine factor for mast cell degranulation (in chapter 1), I tried allergic therapy by using neutralizing antibody against histone H1.

A histone H1-neutralizing Ab, SSV mAb, suppressed antigen-induced degranulation from IgE-sensitized RBL-2H3 cells (Fig. 9). The anti-degranulation activity was also observed in mast cell-driven PCA model mice (Fig. 10), which indicated that SSV mAb treatment directly suppressed mast cell reactions at inflammatory sites. SSV mAb also ameliorated allergic rhinitis-like nasal symptoms and diminished mast cell expansion in nasal mucosal tissues (Fig. 11), while lymphocytes-mediated systemic immune responses including production of antigen-specific immunoglobulins and Th1/Th2 cytokines were intact (Fig. 12), suggesting that the histone H1-targeted therapy directly suppressed mast cell degranulation on allergic disorders. Unexpectedly, SSV mAb did not downregulate serum histone H1 level (Fig. 13A), although it dramatically ameliorated nasal symptoms. By contrast, in this histological staining, I successfully observed that SSV mAb decreased local expression of histone H1 at nasal mucosal tissue (Fig. 13B). Thus SSV mAb neutralized local histone H1 for disturbing positive feedback

loop of type I allergic reactions at local allergic inflammation site, which fulfilled a dramatic anti-allergic activity.

Chapter 3:

Identification of a novel type I allergic reaction inhibitory factor from *Perilla frutescens* and elucidation of its inhibitory mechanisms

1. Introduction

Perilla frutescens is an edible Asian medical herb that possesses capability to reduce inflammatory reactions including asthma[74,75]. It has previously been found that *P. frutescens*-containing diet prevented the exacerbating of skin inflammation in atopy-prone NC/Nga mice. In this *in vivo* study, *P. frutescens* diet inhibited Th2 differentiation, IgE production from B cells, and histamine release from mast cells (unpublished data). *P. frutescens* contains a variety of phytochemicals, especially polyphenols which have been reported to play roles for anti-inflammatory effects[76]. Rosmarinic acid, a reported primary anti-inflammatory factor in *P. frutescens*[77], showed those effects by suppressing IL-4, IL-5 and eotaxin production in bronchial alveolar lavage fluid of mite-sensitized mice[78]. Caffeic acid showed anti-mast cell-mediated inflammatory activity to alleviate compound 48/80-induced skin irritation by decreasing skin histamine content[79]. Luteolin has a potent anti-allergic activity to inhibit mast cell degranulation, and also shows anti-inflammatory activity suppressing IL-1β and TNF-α production from macrophages stimulated with romurtide and LPS, and chemical-induced inflammation, ear edema[80,81]. Apigenin and luteolin suppress degranulation of mast cells and inhibited

IgE production from B cells[82]. There are lots of reports about anti-inflammatory effects of those *P. frutescens*-derived polyphenols, relative contribution and/or hierarchy of those compounds on anti-allergic effect remains to be elucidated.

Type I allergy is a mast cell-dependent inflammatory disease[7]. Allergic symptoms (*e.g.* sneezing, asthma and anaphylaxis) are initially triggered by antigen-driven cross-linking of IgE bound on FcεRI on mast cells. Cross-linking of IgE on mast cells by antigen activates mast cells and induces mast cell degranulation[83]. Proinflammatory chemical mediators including histamine are released upon mast cell degranulation[84,85]. Mechanically, cross-linking of IgE induces sequential phosphorylation of Lyn, Syk, PI3K, PLCγs and Akt and subsequently Ca^{2+} influx via Lyn-Syk-LAT pathway[86].

In this study, I found a hitherto-unrecognized *P. frutescens*-derived flavanone derivative (*Perilla*-derived methoxyflavanone, PDMF) that suppresses IgE-dependent mast cell degranulation. PDMF showed a more potent type I allergic reaction inhibitory activity than those by known *P. frutescens*-derived anti-inflammatory polyphenols. PDMF directly acts on mast cells to negatively regulate FcεRI signaling pathway *in vitro*, and attenuated passive cutaneous anaphylaxis and allergic rhinitis *in vivo*.

2. Materials and methods

2.1. Mice and ethical statements

Five-week-old female BALB/c mice were purchased from Charles River Laboratories Japan, and fed with sterile distilled water and commercial diets *ad libitum* under specific pathogens-free condition at 23 ± 3°C with 12 hrs light-dark cycles. All serum samples were stored at -80°C until analysis. All experiments using mice were carried out using protocols approved by the Animal Studies Committee of Hiroshima University.

2.2. Preparation of hot water extract of Perilla frutescens leaves and its purification with reversed-phase chromatography

Dried powder of *P. frutescens* leaves was provided from Mishima Food Co., Ltd. (Hiroshima, Japan), and preserved with avoiding water and light, at 4°C. The *P. frutescens*-powder (300 g) was extracted with stirring in boiling water (95°C, 2 L) for 1 hr, and then squeezed. The extract was centrifuged at 120 x *g*, for 10 min, and its supernatant was filtrated with filter paper, subsequently concentrated by evaporation, and finally lyophilized. Resultant yield of the hot water extract of *P. frutescens* was 60 g dry weight. The extract (30 g) dissolved in water was fractionated by reversed-phase chromatography with using MCI gel CHP20P (Mitsubishi Chemical, Tokyo, Japan) with sequential elution with 5 times the column volume of water, 4 times the column volume of methanol, and finally with 4 times the column volume of acetone. Each eluant was concentrated by

evaporator and then lyophilized to give 23.9 (for water fraction), 4.0 (for methanol fraction), and, 0.2 g (for acetone fraction), as a dry weight, respectively. The methanol fraction was further fractionated by using a reversed-phase column (Mightysil RP-18 GP column (10 x 250 mm), Kanto Chemical, Tokyo, Japan) under flow of 40% acetonitrile containing 0.01% trifluoroacetic acid with flow velocity to 2.36 ml/min, at 40°C, on high performance liquid chromatography (HPLC) operated with Gilson Uni Point TM LC system Software Version 5.11. Fractions whose retention time between 0 to 10 min (fraction 1), 10 to 20 min (fraction 2) and 20 to 30 min (fraction 3) were respectively collected, and those yields were 1.4, 1.2, and 0.22 g, as a dry weight. The fraction 2 was further fractionated using the reversed-phase column with 30% acetonitrile on HPLC and collected totally to 7 peaks detected by absorbance at 210 nm (Fig. 14B).

2.3. Structural analysis of a Perilla-derived metoxyflavanone (PDMF)

Chemical structure of active component (corresponding to peak 4) was determined by mass spectrometry (MS), nuclear magnetic resonance (NMR), and Fourier transform infrared spectroscopy (FT-IR). Atmospheric pressure chemical ionization (APCI) mass spectrum was measured with LTQ Orbitrap XL mass spectrometer (Thermo Fisher Scientific, MA, USA)[87]. The possible molecular formula was subjected to *in silico* analysis were estimated by using species-metabolite relationship database KNApSAcK (NAIST Comparative Genomics Laboratory: Nara, Japan)[88]. NMR spectra

were recorded with a JEOL Lambda-500 spectrometer equipped with a field gradient apparatus. The chemical shifts were recorded as a δ value on the basis of a residential solvent signal (δ_C 77) or internal standard tetramethylsilane (δ_H 0). FT-IR spectrum was obtained by Spectrum One FTIR spectrometer (Perkin-Elmer) with the attenuated total reflectance (ATR) method. The optical activity of PDMF was analyzed by polarimeter (JASCO DIP-370) and chiral HPLC. The chiral HPLC analysis was performed on a MB-S column (2 x 250 mm, Tokyo Chemical Industry, Tokyo, Japan) with flow velocity to 2.36 ml/min of 20% acetonitrile.

2.4. Mast cell degranulation using RBL-2H3 cells

In vitro IgE-mediated degranulation from RBL-2H3 cells was performed by protocol previously described in chapter 1. 2.6. Briefly, RBL-2H3 cells (6 x 10^4 cells/well) incubated for 8 hrs were sensitized with anti-DNP IgE (0.5 ng/well) for 16 hrs. After PBS washing them, they were incubated in MT buffer containing *P. frutescens*-fractions (100 μl/well); 500 μg/ml hot water extract; 400, 30 or 10 μg/ml fraction for water, methanol or acetone from hot water extract, respectively; 250, 200 or 50 μg/ml fraction 1, 2, or 3 of first round HPLC, respectively; 42, 50, 21, 26, 26, 44, and 83 μg/ml for fraction 1 to 7 of 2nd round HPLC; or 0.54% dimethyl sulfoxide (DMSO) as a vehicle control for 30 min. Subsequently, their degranulation were induced by DNP-BSA (12.5 ng in MT buffer) for 30 min. After stopping the reaction with incubating at 4°C, for 10 min, the supernatant was then

collected by centrifuging at 190 x *g*, for 5 min, at 4°C. The 100% degranulation for each well was estimated from the cell lysate which was prepared with 0.2% triton X-100. Degranulation was evaluated from histamine concentration measured by Histamine EIA kit (Oxford Biomedical Research, Oxford, UK) with a Wallac 1420 ARVOsx Multilabel Counter (Perkin-Elmer, Downers Grove, IL, USA).

2.5. Calculation of half maximal inhibitory concentration (IC_{50}) for degranulation

The mast cell degranulation protocol was same with 2.4, with changing samples to 25, 50, 75, 100, 150, or 300 μM of PDMF or apigenin (EXTRASYNTHESE, Riom, France); 75, 100, 150, 200, 250, or 300 μM of luteolin (EXTRASYNTHESE); 300, 500, 750, or 1000 μM of rosmarinic acid (wako); 300, 500, 600, 700, 800, or 1000 μM of caffeic acid (TCI); 1 μM 4-amino-5-(4-chlorophenyl)-7-(dimethylethyl)pyrazolo[3,4-*d*]pyrimidine (PP2, sigma); or 0.54% DMSO as a vehicle control. Half maximal inhibitory concentration (IC_{50}) was calculated with regarding histamine release level of IgE+Ag as no inhibition (0%) and those of IgE as completely inhibition (100%), with using at least three points of significantly inhibition percentage by samples as compared with IgE+Ag (except for 50 μM of PDMF, $P = 0.054$).

2.6. Measurement of intracellular Ca^{2+} influx into RBL-2H3 cells

Calcium (Ca^{2+}) influx into RBL-2H3 cells through FcεRI-mediated signal transduction of degranulation was analyzed according to the method described previously with some modifications[89]. RBL-2H3 cells were seeded and sensitized in a black 96-well flat bottom plate as following procedure in 2.4, they were then incubated with fluo4-AM (Dojin Chemical Laboratories, Kumamoto, Japan) for 1 hr, at 37°C. After twice cell washing with PBS, they were incubated with 100 or 300 μM PDMF; or 0.54% DMSO as a vehicle control for 30 min. The intracellular Ca^{2+} level was measured as 485/535 nm (Excitation (Ex)/Emission (Em)) every 1 min, for 10 min, from just after stimulating the cells with DNP-BSA.

2.7. Cytotoxicity analysis

RBL-2H3 cells were incubated and sensitized as described in 2.4., subsequently washed with PBS, incubated with 100, 300 or 500 μM PDMF; or 0.54% DMSO as a vehicle control for 1 hr. After washed twice with PBS, the cells were removed from the culture plate by incubation with trypsin-EDTA (Thermo) and harvested by centrifugation at 190 x *g*, for 5 min. The viable cells were counted by trypan blue-exclusion assay using a hemocytometer.

2.8. PCA model mice

Synthetic PDMF was obtained as a custom synthesis product, supplied by TCI, to evaluate various *in vivo* activities. Mice were orally administered with 5 mg PDMF (n = 9), apigenin (n = 6), or 3% DMSO in 5% ethanol as a vehicle control (n = 9) every day for 8 days. An anti-DNP IgE (150 ng/10 μl) or PBS blank was intradermally injected into the right or the left ear at day 7, respectively. As a sham control, PBS was injected into both right and left ears (n = 10). 24 hrs later, their PCA was induced by intravenous injection of 200 μg DNP-HSA in 100 μl PBS containing 0.5% Evans blue. After 30 min, severity of PCA reaction was evaluated by quantification of Evans blue leaked into ears which was extracted with formamide overnight at 63°C. The level of Evans blue was measured by absorbance at 595 nm with a Wallac 1420 ARVOsx Multilabel Counter.

2.9. Preparation of Cryptomeria japonica pollen (CJP) extract and its biotinylation

Pollens were collected from *Cryptomeria japonica* by myself, in Hiroshima, Japan, and stored at -80°C until use. To prepare its extract, 150 g pollen was stirred in 6 L PBS, at 4°C, for 4 hrs, and centrifuged at 6800 x *g*, for 30 min. The supernatant was applied into ammonium sulphate precipitation method with 80% saturated-ammonium sulphate. Collected precipitate was dissolved in distilled water and dialysed overnight with stirring at 4°C. It was centrifuged at 6500 x *g*, for 30 min, and then its

supernatant was filtered with 0.22 μm filter unit to obtain crude Japanese cedar pollen extract. The resultant extract was lyophilized and stored at -80°C until use. To biotinylate CJP, 10 mM biotin (30 μl, Thermo) was added to 1 mg/ml CJP (1 ml) and incubated for 30 min at room temperature. Then the reagent was ultrafiltrated with Amicon Ultra 3K (Merck Millipore), and 3 times wash with PBS. 4.93 molecule of biotin bound a CJP evaluated by HABA solution (Thermo).

2.10. Japanese cedar pollinosis model mice

Japanese cedar pollinosis model mice were set up by based on immunization with the CJP and intranasal challenge with pollen. BALB/c mice were orally administrated with PDMF (1.5 or 0.75 mg, each n = 10), apigenin (1.5 mg, n = 10) or 5% ethanol containing 3% DMSO as a vehicle control (n = 20) every day during the test. They were intraperitoneal immunized with 100 μg CJP solution (100 μl) containing with 1 mg adjuvant alum (Thermo) at day 1 and 7. As a sham control for immunization (n = 10), PBS/alum was intraperitoneally injected. 0.5 mg/20 μl pollen solution was intranasally challenged after 1-2 hrs from oral administration, every day during day 17-23. To evaluate their nasal symptoms, their sneezing were counted for 5 min, after intranasal challenge every day. After the last nasal challenge, mice were sacrificed and collected their fundus blood. Those blood were mixed with 3 μmol EDTA-2Na, and centrifuged at 10,000 x *g*, for 10 min, at 4°C, finally its supernatant were collected as serum.

2.11. ELISA for total and CJP-specific immunoglobulins

The antibodies for ELISA were purchased from Nippon Becton Dickinson Company, Ltd. (Tokyo, Japan). To evaluate serum levels of antibodies, 2 μg/ml purified anti-mouse IgE for total and specific IgE or 100 μg/ml CJP for IgG1 and IgG2a were respectively coated on 96-well microplates (Nalgene Nunc International) and the plates were incubated overnight at 4°C. After plate washing with 0.05% Tween 20 containing PBS (PBST) repeated 3 times, the plates were blocked with blocking buffer (5% skim milk dissolved in PBS) for 2 hrs, at 37°C. After plate washing with PBST repeated 3 times, serum samples (50-fold diluted with blocking buffer for total IgE, 15-fold diluted for CJP-specific IgE, 4000-fold diluted for CJP-specific IgG1 and 20-fold diluted for IgG2a) were applied to each well and the plates were incubated overnight at 4°C. After plate washing with PBST repeated 3 times, the plates were incubated with 2 μg/ml biotin conjugated anti-IgE antibody for total IgE, 2 μg/ml biotin-conjugated CJP for CJP-specific IgE, 4 μg/ml biotin conjugated anti-IgG1 antibody for CJP-specific IgG1, 2 μg/ml biotin conjugated anti-IgG2a antibody for CJP-specific IgG2a, for 2 hrs, at 37°C. After plate washing with PBST repeated 6 times, the plates were incubated with 1 μg/ml Streptavidin, Alkaline Phosphatase Conjugate (1000-fold diluted with blocking buffer: Thermo) for 1 hr at 37°C. Attophos substrate (Promega K.K.: Tokyo, Japan) was applied to each well and measured fluorescent of Ex 453/Em 535 nm by

a Wallac 1420 ARVOsx Multilabel Counter.

2.12. Immunoblot analysis of FcεRI-mediated signal transduction molecules for degranulation

RBL-2H3 cells expresses FcεRI, and shows IgE-mediated degranulation *via* FcεRI-dependent pathway[90,91]. RBL-2H3 cells were seeded in 5 ml cell culture dish at 1.5 x 10^6 cells per plate, for 8 hrs. The cells were sensitized with 9 ng anti-DNP IgE in 5 ml medium, for 16 hrs, and followed by incubation with 2.5 ml 100 or 300 μM PDMF or 1 μM PP2 for 30 min, and then added with 563 ng/250 μl DNP-BSA. The cells were further incubated for 10 min, at 37°C. After washing the cells twice with chilled PBS. The cells were dissolved with 100 μl/ lysis buffer (50 mM NaCl, 1 mM EDTA, 50 mM NaF, 30 mM $Na_4P_2O_7$, 2 μg/ml aprotinin, 5 mg/ml Pefabloc SC, a protease inhibitor cocktail (Roche Diagnostics, Tokyo, Japan) and 1% phosphatase inhibitor cocktail (Nacali tesque, Kyoto, Japan) at 4°C, for 30 min. The cell lysates were harvested by cell scraper and then sonicated to completely dissolve proteins. These supernatants were corrected after centrifugation with 14,000 x *g*, at 4°C, for 15 min, and protein concentration of these samples were measured by DC-protein assay kit (Bio Rad, California, USA). The cell lysates were mixed 1:1 with two-fold-concentrated sample buffer containing 0.1 M Tris-HCl, 4% SDS, 20% glycerol, 10% 2-mercaptoethanol, 1% bromophenol blue at pH6.8, and incubated at 100°C, for 8 min. Each 60 μg proteins in cell lysate were separated by sodium lauryl sulfate

polyacrylamide gel electrophoresis (SDS-PAGE). After SDS-PAGE, the separated proteins were transferred onto a PVDF membrane and the membrane was incubated in TBST (50 mM Tris hydroxymethyl aminomethane, 150 mM NaCl, and 0.1% tween-20, pH7.5) supplemented with 5% non-fatty acid skim milk for 1 hr, at 25°C. Then, the membrane was incubated with primary antibodies (2,500-fold diluted anti-Syk pAb, 1,250-fold diluted anti-pSyk mAb (Y525/526), 2,500-fold diluted anti-PI3Kp55 mAb, 5,000-fold diluted anti-PI3Kp85 mAb, 1,259-fold diluted anti-pPI3Kp55 (Y199)/p85 (Y458) pAb, 2,500-fold diluted anti-Akt pAb, 2,500-fold diluted anti-Akt/PKB pAb (S473), 1,250-fold diluted anti-PLCγ1 mAb, 1,250-fold diluted anti-pPLCγ1 pAb (Y783), 1,250-fold diluted anti-PLCγ2 pAb, or 1,250-fold diluted anti-pPLCγ2 pAb (Y759) antibody; Cell Signaling Technology Japan, Tokyo, Japan) overnight, at 4°C. The positive bindings for each antibody were detected by 5,000-fold diluted horseradish peroxidase (HRP)-linked anti-rabbit IgG, polyclonal antibody for 1 hr, at 25°C, and followed by visualized by using an ECL Plus Western Blotting Detection System (GE Healthcare Bio-Sciences, Tokyo, Japan).

2.13. Statistical analysis

Data contained standard deviation expressed as mean ± S.D. Non-paired Student's t-test was used to assess statistical significance of difference compared to corresponding controls. Statistical significance was defined as $p < 0.05$. Statistical analysis among 4 groups was performed by

Kruskal-Wallis H-test with post hoc analysis using a Mann-Whitney U-test with Bonferroni correction (two tails, non-parametric).

3. Results

3.1. Isolation of a novel anti-degranulation factor from P. frutescens

Previous reports indicated that hot water extract of *P. frutescens* showed anti-allergic activity[92,93]. To confirm this, soluble component of *P. frutescens* leaves extracted with hot water was applied into *in vitro* degranulation assay with using RBL-2H3 cells. The extract significantly inhibited IgE-mediated histamine release (histamine release of IgE+Ag was 37.0 ± 1.5%, 500 μg/ml hot water extract was 23.1 ± 2.5%; Fig. 14A). To explore anti-degranulation factor, the hot water extract was fractionated by reversed-phase chromatography with water, methanol and acetone as eluants. I found that methanol fraction but not water or acetone fractions showed potent anti-degranulation activity (sample concentration, histamine release percentage ± S.D.; water fraction (400 μg/ml, 36.8 ± 4.9%), methanol fraction (30 μg/ml, 19.2 ± 2.6%), acetone fraction (10 μg/ml, 31.4 ± 2.3%)). The lowest histamine releasing by the water and acetone fractions were 29.7 ± 2.8% (at 500 μg/ml) and 24.6 ± 4.7% (at 250 μg/ml), respectively. Fractionation of the methanol fraction by the first round of reversed-phase HPLC concentrated almost the anti-allergic activity into a fraction of retention time (RT) 10-20 min (sample concentration, histamine release percentage ± S.D.; RT 0-10 min (250 μg/ml, 30.2 ± 3.7%), RT 10-20 min (200 μg/ml, 21.3 ± 3.6%), RT 20-30 min (50 μg/ml, 30.8 ± 2.9%). The fraction of RT 20-30 min showed no activity even 500 μg/ml (31.7 ± 4.6%).

In further purification of the anti-degranulation factor by the second

round of reversed-phase HPLC, total of 7 peaks were detected at absorbance of 210 nm (Fig. 14B). Those peaks were applied to *in vitro* degranulation assay with 0.54% DMSO as a vehicle control. I found that peak 4 showed the most potent histamine releasing inhibitory activity compared with the other peaks (histamine release percentage ± S.D.; IgE+Ag (41.8 ± 2.4%), peak 4 (19.9 ± 1.3%); Fig. 14C). And in this purification procedures of peak 4 was estimated as more than 95%, confirmed by HPLC with multiple absorbance (data not shown).

The retention time of peak 4 on reversed-phase HPLC (13.0 min) was distinguished from those of known *P. frutescens*-derived anti-allergic polyphenols including rosmarinic acid, caffeic acid, apigenin and luteolin; they were detected as a distinct peak respectively at 6.2, 5.0, 19.0 and 10.7 min of retention times (Fig. 14E; octa decyl silyl (ODS) 4.6 x 250 mm; eluent: 40% acetonitrile containing 0.1% trifluoroacetic acid). These results suggested that peak 4 was a unidentified type I allergic reaction inhibitory factor in the *P. frutescens* extract.

3.2. Structural elucidation of an anti-degranulation factor in peak 4

The ultraviolet-visible spectrum of the active peak 4 (Fig. 14D, λ_{max} = 291 and 351 nm) is a characteristic of flavanones such as naringenin[94]. IR spectrum of peak 4 (Fig. 15A) indicated the presence of α,β-unsaturated carbonyl (1580-1660 cm^{-1}) and hydroxyl (3200-3500 cm^{-1}) groups. The high-resolution positive atmospheric pressure chemical ionization-mass

spectrometry (APCI-MS) analysis of peak 4 showed the specific peak at 301.107 m/z, establishing its molecular formula to be $C_{17}H_{16}O_5$ (Fig. 15B). Its MS/MS spectrum showed the single peak at 197.044 m/z (Fig. 15C), which was the retro-Diels Alder reaction of characteristic of flavonoids (Fig. 15D)[95]. Candidate compounds of peak 4 were estimated as methoxyflavanone by using species-metabolite relationship database KNApSAcK (NAIST Comparative Genomics Laboratory: Nara, Japan) [88], and peak 4 was referred to *Perilla*-derived methoxyflavanone, PDMF.

The ^{13}C NMR of PDMF indicated the presence of 15 carbons (Fig. 16A), which were classified by distorsionless enhancement by polarization transfer (DEPT) spectrum as five deshielded methine (δ_C 80.0, 89.8, 126.3, 128.8, and 128.9), one methylene (δ_C 45.8), two deshieled methyl (δ_C 56.2 and 56.4), and seven quaternary carbons (δ_C 105.9, 127.7, 138.3, 149.4, 152.4, 155,0 and 189.2). Two methine signals (δ_C 126.3 and 128.9) were enriched in its spectrum, possibly due to the signal duplication. Its ^1H NMR spectrum showed 16 protons (Fig. 15B), two double-doublet protons (δ_H 2.85 and 3.10), two deshielded methyl protons (δ_H 3.92 and 3.98), one deshielded double-doublet proton (δ_H 5.49), one singlet methane proton (δ_H 6.19), and five aromatic protons (δ_H 7.39-7.48). Based on their chemical shift, two methyl groups were assigned to be methoxy moieties. In addition, the ^1H coupling pattern together with the ^{13}C chemical shift indicated the presence of a non-substituted phenyl groups. Its ^1H and ^{13}C NMR assignments were summarized in Table 2.

The connectivity was clarified by two-dimensional NMR techniques including double quantum filtered-correlated spectroscopy (DQF-COSY), heteronuclear multiple quantum coherence (HMQC), and heteronuclear multiple-bond connectivity (HMBC) (Fig. 16C). First, the Ph-C2-4 structural fragment was established based on correlation of C-2 deshielded double-doublet proton (δ_H 5.49) with a phenyl carbon (δ_C 126.3), C-3 double-doublet methine protons (δ_H 2.85 and 3.10), and a C-4 deshielded quaternary carbon (δ_C 189.2). The four singlet proton signals at δ_H 5.07 (exchangeable OH proton), 3.92 (methoxy), 3.98 (methoxy), 6.19 (aromatic/olefin proton) are assigned at A-ring in flavanone skeleton. They substitutes at C-8 (δ_C 5.49), C-7 (δ_C 56.4), C-5 (δ_C 56.2), and C-6 (δ_C 89.8), respectively. The substituted positions were determined from strength of long-range correlations from C-6 proton to C-5 and C-7 carbons, to C-4a (δ_C 105.9) and C-8 carbons, respectively. The position of methoxy group was determined by nuclear Overhauser effect (NOEs), in which H-6 proton showed similar NOE values with two methoxy protons attached at C-5 and C-7 in same strength (41.1% and 40.4%, respectively). Based on these spectroscopic analyses, the active peak 4 was determined to be 8-hydroxy-5,7-dimethoxyflavanone (Fig. 16D). PDMF harbors the chiral center at C-2 carbon, however, whose optical rotation value was almost 0 (c = 4.24 in $CHCl_3$), suggesting this compound was racemic. This optically negative property was also supported by chiral HPLC analysis, in which two peaks were detected at 19.7 and 24.7 min in 1:1 ratio (Fig. 16E).

3.3. PDMF shows a more potent anti-degranulation activity as compared with those of known P. frutescens-derived polyphenols

To determine the hierarchy of anti-degranulation activity among PDMF and known *P. frutescens*-derived polyphenols including rosmarinic acid, luteolin, apigenin and caffeic acid, they were subjected to IgE-mediated mast cell degranulation assay. Half maximum of histamine release inhibitory concentration (IC_{50}) of PDMF was determined as 68.5 μM, which was calculated with regarding IgE as 100% inhibition and IgE+Ag as 0% inhibition of degranulation (Fig. 17A). By contrast, IC_{50} of *P. frutescens*-derived polyphenols were 96.8, 174.1, no effect and 620.4 μM for apigenin, luteolin, rosmarinic acid and caffeic acid, respectively (Fig. 17C). In addition, maximum inhibition rate of PDMF was 83.8 ± 0.86% at 100 μM, while those of the other polyphenols were lower (apigenin; 100 μM, 50.4 ± 1.68%, luteolin; 200 μM, 62.9 ± 1.87%, caffeic acid; 700 μM, 58.9 ± 2.12%). Viability assay by trypan blue exclusion test revealed that PDMF has no cytotoxicity against even 300 μM (Fig. 17B). These data suggested that the PDMF showed a more potent anti-degranulation activity than *P. furtescens*-derived polyphenols.

3.4. PDMF suppresses PCA as well as nasal symptoms in a murine model of Japanese cedar pollinosis

To evaluate *in vivo* anti-allergic effect of PDMF, PDMF was orally

administrated to PCA model mice (Fig. 18A) whose anaphylaxis was demonstrated to be fulfilled by mast cell-dependent mechanisms [83]. PDMF showed significant suppression of anaphylactic reaction (inhibition 53.4 ± 19.5%) comparable to apigenin (72.6 ± 25.8%, no significant difference between PDMF and apigenin was noted: Fig. 18B, C). These results suggested that PDMF also inhibited mast cell degranulation *in vivo* for suppression of type I allergic responses.

In vivo anti-allergic potency of PDMF was further evaluated by prophylactic administration to Japanese cedar pollinosis model mice upon intraperitoneal immunization and nasal sensitization with Japanese cedar pollen allergens (Fig. 19A). Oral administration with PDMF (1.5 mg/day or 0.75 mg/day shown as 1/2 PDMF) significantly suppressed the development of rhinitis-like nasal symptoms as compared with those of sham-treated mice, while apigenin (1.5 mg/day) failed to suppress the symptom at day 7 (Fig. 19B). In contrast, PDMF had no effect on total IgE levels and Japanese cedar pollen (CJP)-specific immunoglobulin titers including IgE, IgG1, and IgG2a (Fig. 19C-G). Taken together, PDMF directly downregulates IgE-mediated mast cell reaction without affected on systemic immune response.

3.5. PDMF inhibits Akt-phosphorylation and intracellular Ca^{2+} influx in mast cell degranulation signaling pathway

To elucidate mechanisms of PDMF on intracellular signaling pathway

via FcεRI, cell lysate of PDMF-treated RBL-2H3 cells after IgE-mediated degranulation was analyzed by immunoblotting with each signaling molecule-specific antibodies. PDMF downregulated phosphorylation of Akt without affecting FcεRI-proximal signals including Syk, PLCγs and PI3K subunits (p55 and p85) (Fig. 20A). In addition, I found that PDMF significantly suppressed Ca^{2+} influx as a dose dependent manner (Fig. 20B). These results suggested PDMF showed anti-degranulation activity by downregulation of Akt activation and Ca^{2+} influx (Fig. 20C).

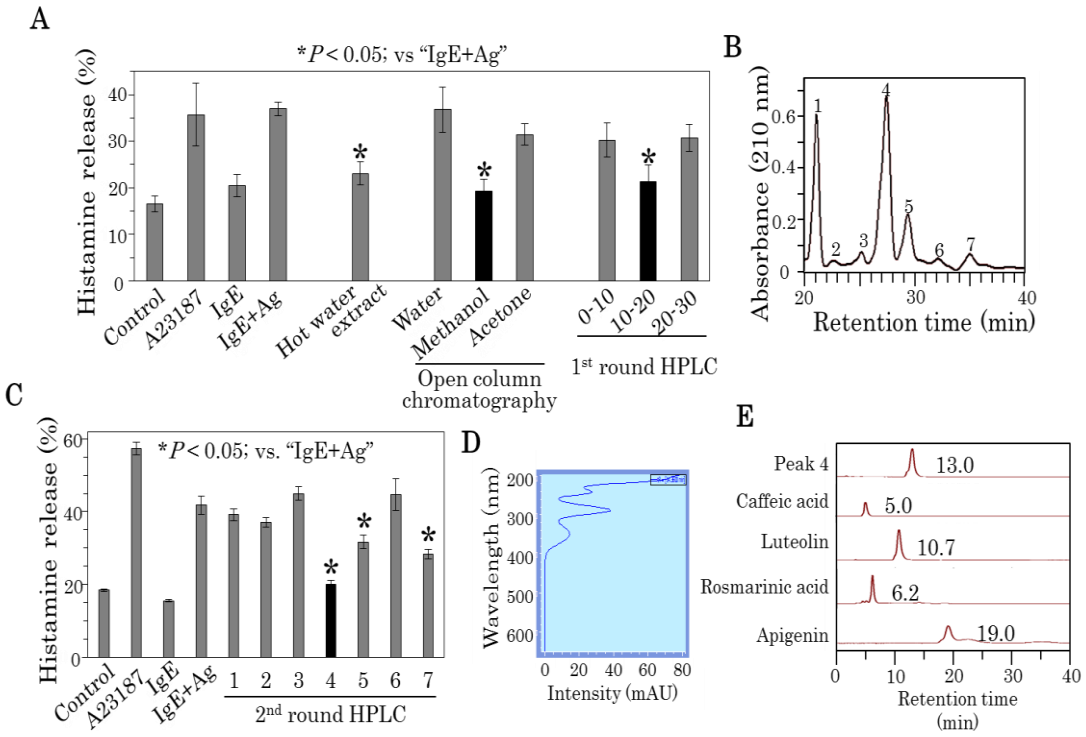

Fig. 14. Purification and isolation of an anti-degranulation factor from P. frutescens extract with evaluating those activities in IgE-mediated mast cell degranulation assay. (A) Calcium ionophore A23187 was a positive control for degranulation. *P. frutescens* hot water extract, its fractionations or 0.54% DMSO as a vehicle control were driven into RBL-2H3 degranulation assay, and whose histamine concentration were measured by histamine EIA kit and shown with the mean ± S.D. (B) A spectrum of the second round of reversed-phase HPLC whose sample was fraction 2 of the first round-HPLC. (C) The histamine releasing driven with the isolated peaks of the second round-HPLC in abundance ratio. Data indicated the mean ± S.D. (D) The ultraviolet-visible of peak 4 absorbance. (E) HPLC spectrums of peak 4 and those of the known anti-allergic polyphenols on reversed-phase HPLC with analysis column.

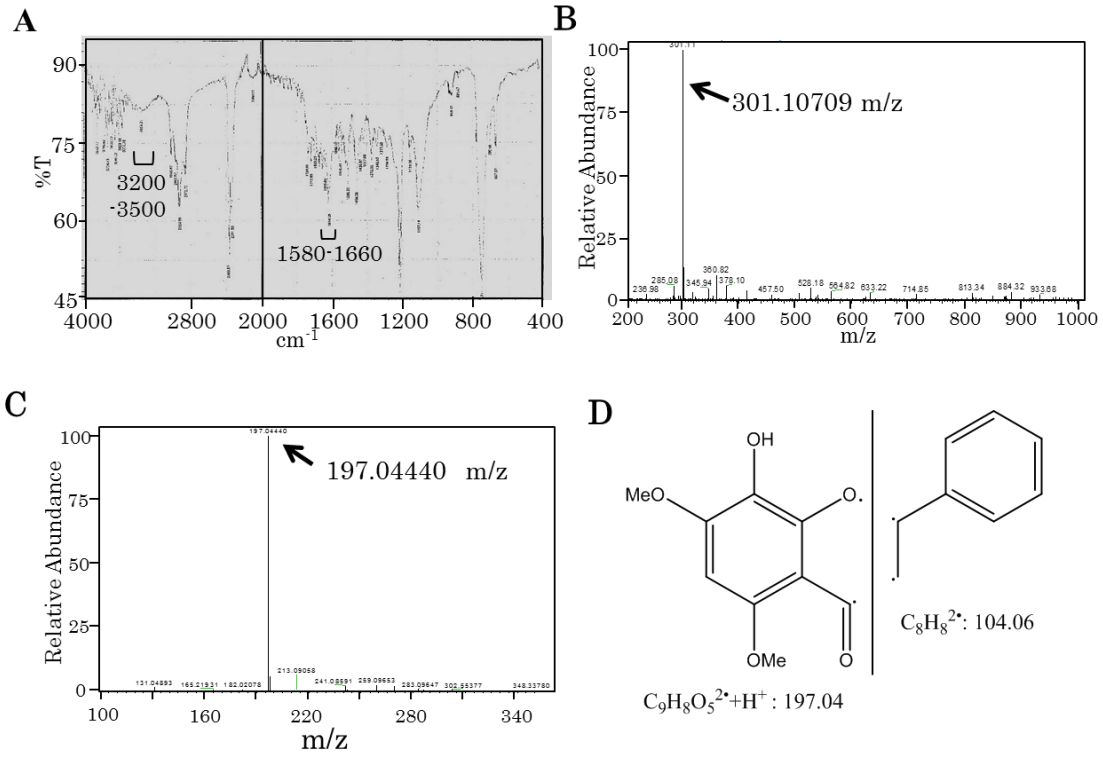

Fig. 15. Estimation of candidate structure of the anti-degranulation peak 4 by IR and MS analyses. (A) IR spectrum of peak 4. (B) MS spectrum. (C) MS/MS spectrum. (D) Retro Dields-Alder reaction of the candidate flavanone of peak 4 in MS/MS analysis.

Table 2. NMR data of 8-hydroxy-5,7-dimethoxyflavanone in $CDCl_3$[a-c]

Position	δ_H (multiplicity, *J*[Hz])	δ_C (multiplicity)
2	5.49 (dd, *J*=13, 2.8)	80.0 (d)
3	2.85 (dd, *J*=17, 3.1) 3.10 (dd, *J*=17, 13)	45.8 (t)
4	-	189.2 (s)
4a	-	105.9 (s)
5	-	152.5 (s)
6	6.19 (s)	89.8 (d)
7	-	155.0 (s)
8	-	127.7 (s)
8a	-	149.4 (s)
1'	-	138.4 (s)
2'	7.43-7.48 (m)	126.3 (d)
3'	7.39-7.48 (m)	128.9 (d)
4'	7.39-7.48 (m)	128.8 (d)
5'	7.39-7.48 (m)	128.9 (d)
6'	7.43-7.48 (m)	126.3 (d)
5-OMe	3.98 (s)	56.2 (q)
7-OMe	3.92 (s)	56.4 (q)
8-OH	5.07 (s)	-

[a]Spectra were recorded at 500 MHz for ^1H and 125 MHz for ^{13}C.

[b]The residential solvent signal (δ_C 77) and internal standard tetramethylsilane (δ_H 0) were used as a reference.

[c]Multiplicity; s, singlet; d, doublet; dd, double of doublet; t, triplet; q, quartet; m, muitiplet.

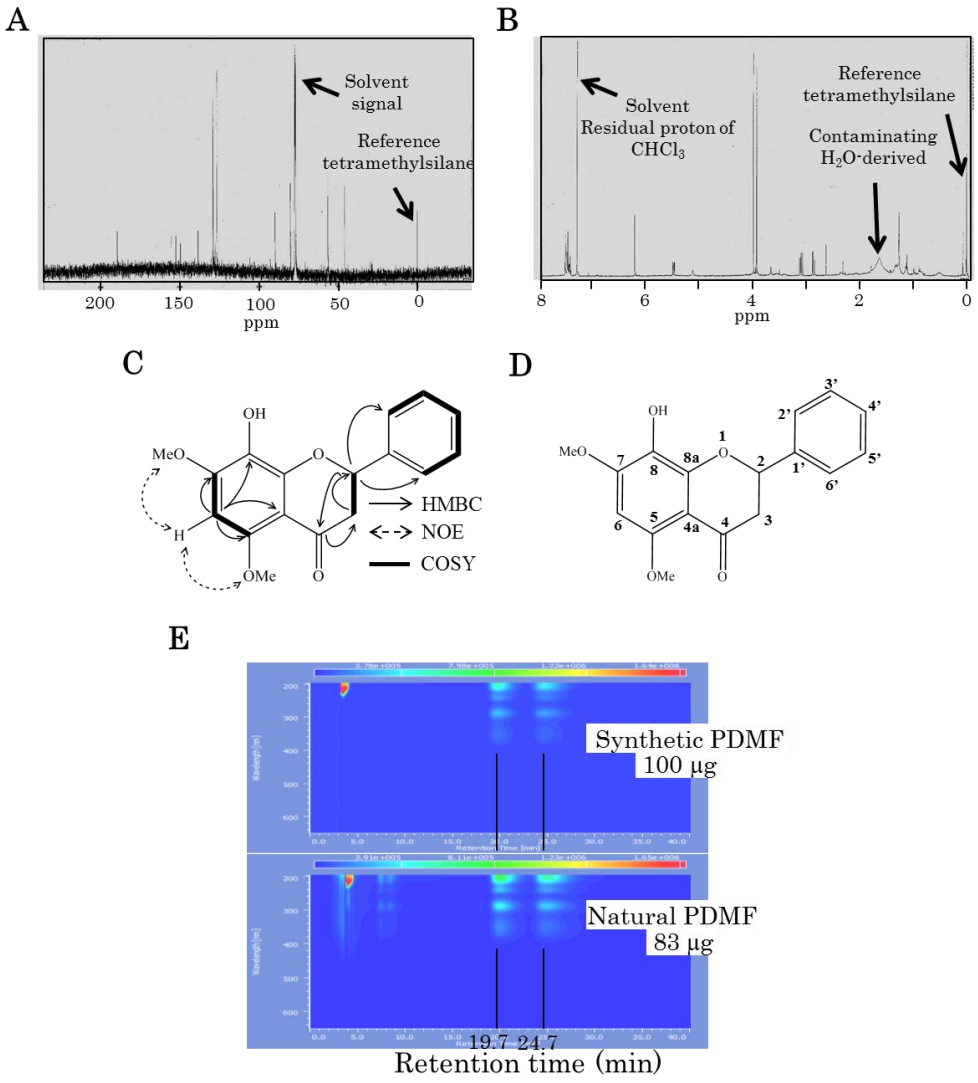

Fig. 16. Structural analyses of PDMF with ^{13}C and ^{1}H NMR, two-dimensional NMR and chiral HPLC. (A) The chemical shifts were recorded as a δ value (ppm) on the basis of a residential solvent signal (δ_C 77) or an internal standard tetramethylsilane (δ_H 0). ^{13}C or ^{1}H NMR spectrum of PDMF were shown in A or B, respectively. (C) The key correlations were shown each arrow. (D) The chemical structure of PDMF identified as 8-hydroxy-5,7-dimethoxyflavanone. (E) Chiral HPLC analysis of PDMF demonstrated their racemic body.

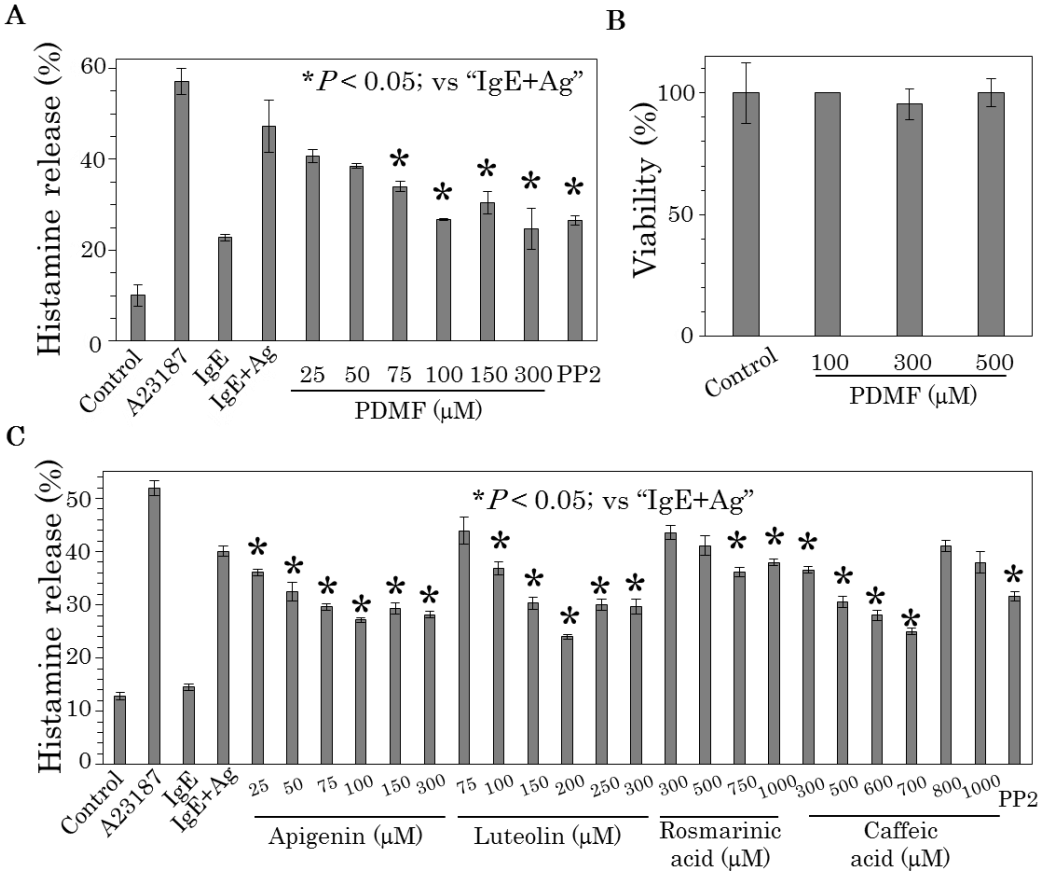

Fig. 17. PDMF showed dose-dependent anti-histamine releasing activity from RBL-2H3 without cell toxicity. IgE-mediated degranulation driven with PDMF (A) or known *P. frutescens*-derived polyphenols (C), were shown with the mean ± S.D., respectively. (B) After cell incubation with PDMF or vehicle, the viable cell were counted by trypan blue-exclusion assay using a hemocytometer. Viability was calculated with the mean count of control vehicle as 100%. Each bar shows mean ± S.D.

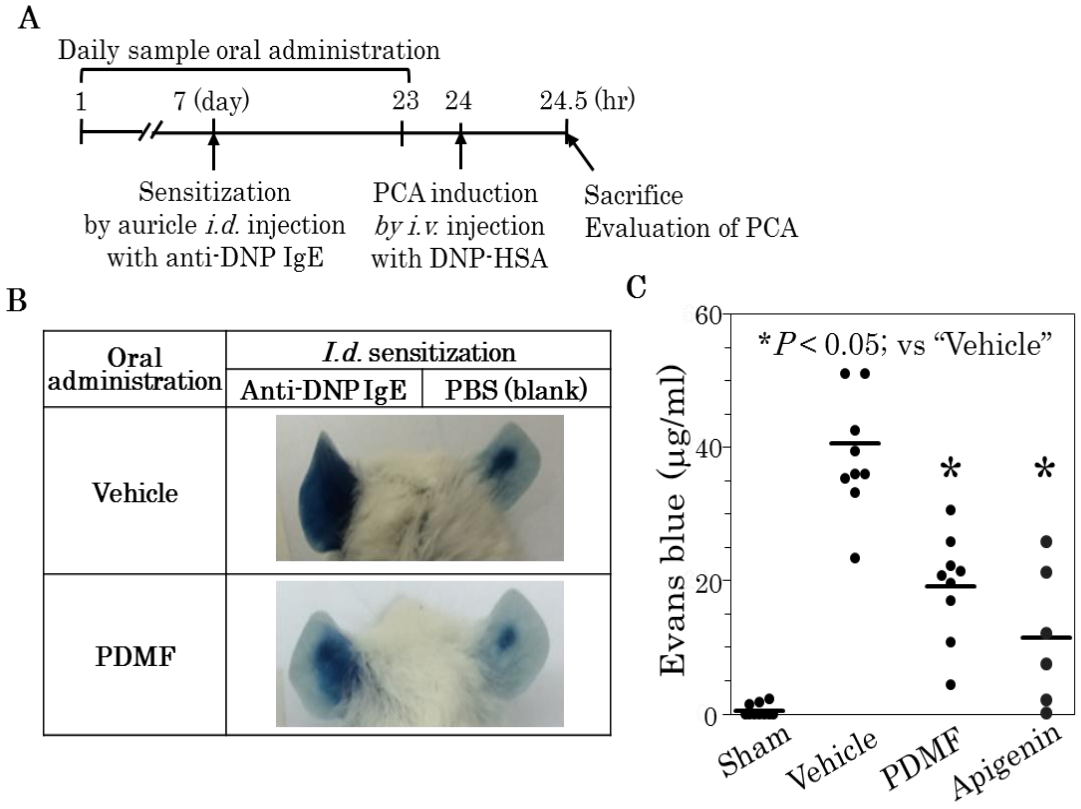

Fig. 18. PDMF suppressed mast cell-dependent passive cutaneous anaphylaxis. (A) A scheme of oral administrating with PDMF, ear sensitization by intradermal (*i.d.*) injection with anti-DNP IgE, PCA induction by intravenous (*i.v.*) injection with DNP-HSA and evaluation the PCA severity on mice. (B) The representative visible data of PCA, anaphylaxis induced Evans blue extravasation into their ears. (C) Each symbol shows an individual Evans blue extracted from their ears (each data subtracted those of right ear as a blank).

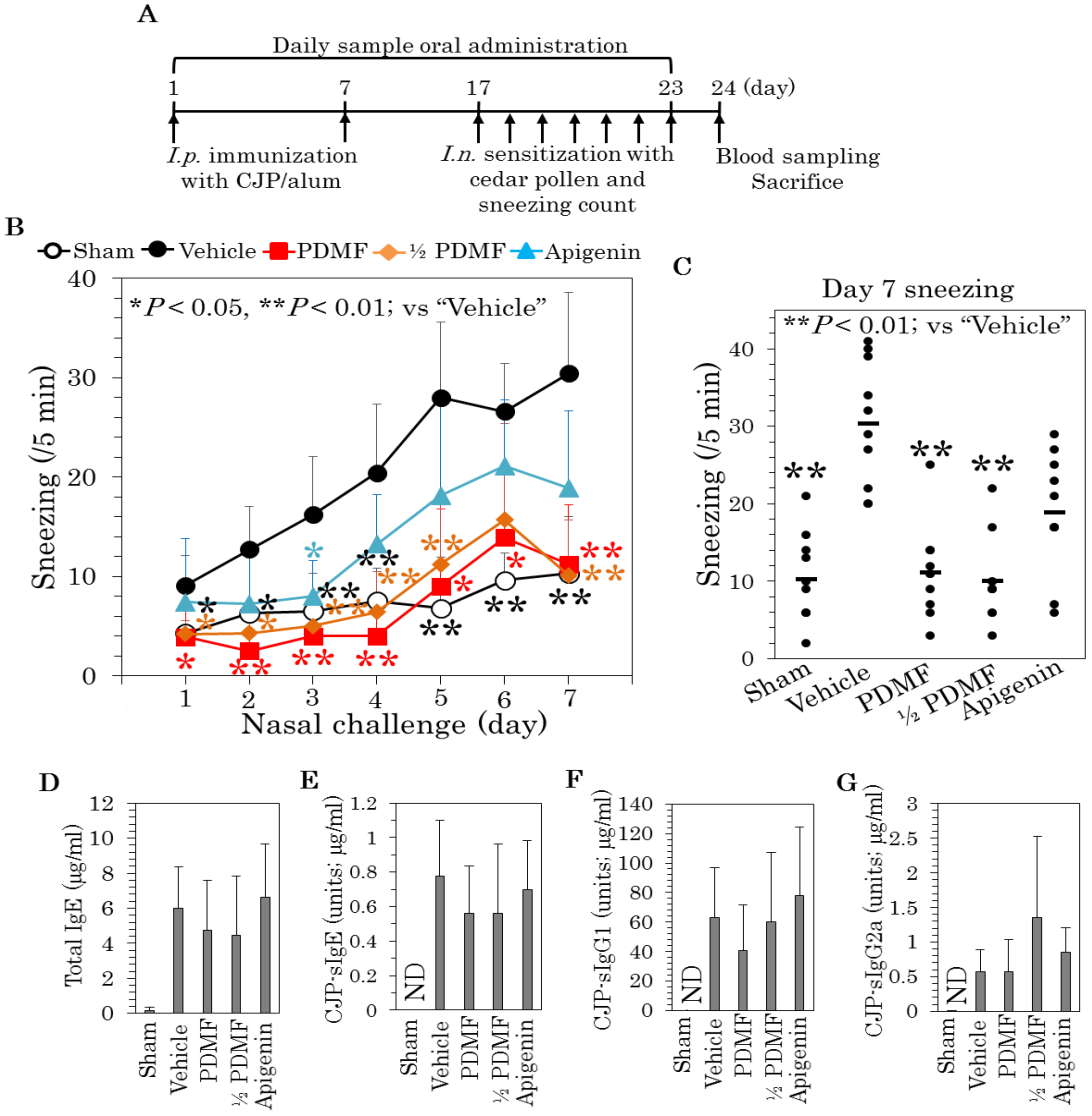

Fig. 19. Allergy-preventive effect of PDMF in Japanese cedar pollinosis. (A) A scheme of oral administration of PDMF (1.5 mg/day or 0.75 mg/day (1/2 PDMF)), apigenin (1.5 mg/day) or 3% DMSO in 5% ethanol as a vehicle control, *i.p.* immunization with cedar pollen extract, intranasal (*i.n.*) challenge with cedar pollen and evaluation of nasal symptom. (B) The nasal symptom evaluated sneezing after nasal challenge. (C) The sneezing after the last nasal challenge (at day 7). Each symbols indicates an individual count of sneezing. Bars shows mean value. (D) Serum immunoglobulin level of total IgE. (E-G) OVA-specific titer of serum IgE, IgG1 and IgG2a, respectively. Data shows mean ± S.D.

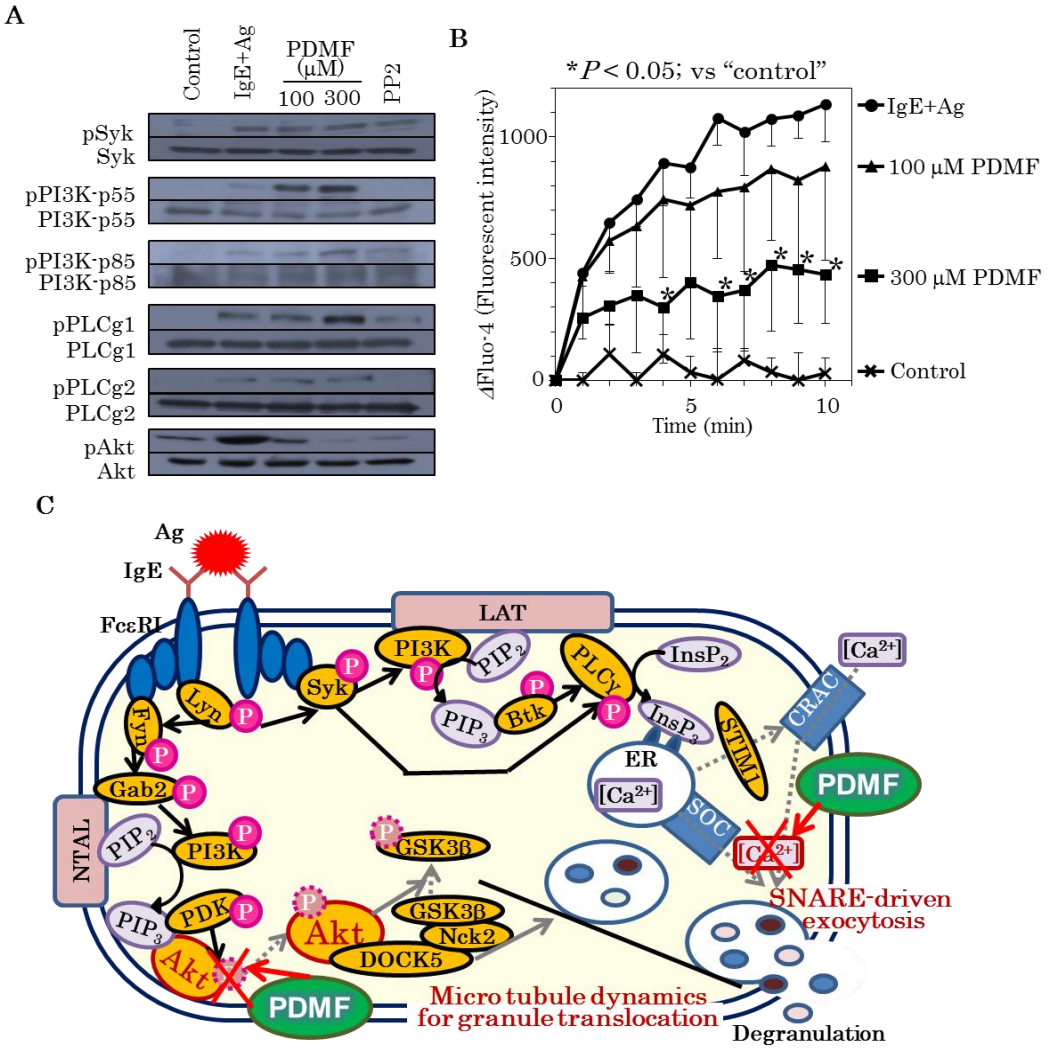

Fig. 20. PDMF suppressed Akt-phosphorylation and Ca^{2+} influx on the FcεRI dependent intracellular signaling pathway. (A) The cell lysate of PDMF-treated RBL-2H3 cells after IgE-mediated degranulation was electrophoresed and then translated into membrane, finally immunoblotted with degranulation signaling molecule-specific antibodies for evaluation of its phosphorylative activating level. As a positive control, Src kinase inhibitor, PP2 (1 μM) was analyzed. Figure was shown representative WB result. (B) Ca^{2+} influx was real time measured by calcium kit-flou 4 with Ex 485/Em 535 nm fluorescence, 0 min meaning as just time of DNP-BSA applying. Data indicates mean ± S.D. (C) Effect points of PDMF on FcεRI-dependent signal transduction.

4. Discussion

In this chapter, I explored a novel potent anti-type I allergic phytochemical from *P. frutescens* with using *in vitro* mast cell degranulation assay of the *P. frutescens*-derived fractions, and finally identified to be 8-hydroxy-5,7-dimethoxyflavanone, termed as PDMF. 8-hydroxy-5,7-dimethoxyflavanone had been isolated from *Piper hispidium*[96] without any biological activities. PDMF may have the other effect against inflammation, because its derivative flavanone whose structure was much similar with PDMF, 8-hydroxy-6,7-dimethoxyflavanone was recently reported as a new anti-inflammatory factor from *P. frutescens*, which inhibited nitric oxide production in IL-1β treated hepatocytes[97].

Kawashima H, *et al* (2016)[98] reported apigenin and luteolin resided in 55 or 35 mg/kg-dry *P. frutescens* leaf, however, on the first round HPLC, the active fraction 2 did not contain known *P. frutescens*-derived anti-degranulation polyphenols. Considered that the resultant yield of PDMF was 100 mg/kg-dry leaf, PDMF may be the most abundant anti-type I allergic compound. The structure-anti-degranulation relationship of flavonoids had been analyzed by Matsuda H, *et al* (2002)[99] among 52 flavonoids including 4 flavanone tested. They referred either a double bound at C-2-3, or hydroxyl group at C-5, -6 or -7 as important modification of anti-degranulation activity, in which apigenin (IC_{50}; 6.0 μM) and luteolin (IC_{50}; 3.0 μM) showed much potent anti-degranulation activity with considering an index of degranulation as β-hexosaminidase activity. By

contrast, PDMF lied out of their rules and showed more potent activity than both apigenin and luteolin, in our experimental conditions (Fig. 17). The possible for differential stracture-activity relationship among PDMF and apigenin, luteolin is that anti-allergic mechanism of PDMF is distinct from those of the known flavonoids. As shown Fig. 20A, PDMF inhibited Akt-phosphorylation without affecting Syk, while flavonols and flavones (including apigenin and luteolin) inhibits Syk activation[100]. In fact, the sufficient structure-anti-degranulation activity relationship remains to be clarified because each group (*e.g.* flavone, flavanone) may effect *via* their specific mechanisms, respectively. According to the inhibition of Akt phosphorylation potency of naringenin (a member of flavanone)[101], flavanone may enhances PIP_3 reductase such as phosphatase and tensin homolog deleted from chromosome 10 (PTEN) and Src homology 2 domain-containing inositol 5' phosphatase (SHIP) to inactivate Akt[102]. Future work is needed to elucidate the necessary structure in PDMF using its derivatives and anti-allergic flavanones including naringenin[101], eriodictyol[103] and newly found 8-hydroxy-6,7-dimethoxyflavanone[97].

As Shown in Fig. 18 and 19, PDMF significantly prevented the development of PCA as well as Japanese cedar pollinosis-like nasal symptoms, suggesting that PDMF is a remarkable anti-type I allergic phytochemical from *P. frutescens*. The future study is needed that elucidation of internal kinetics of PDMF such as absorption.

General conclusions

Allergy is a world-wide social problem, and current therapeutic strategies cannot halt the explosion of allergic patients. Moreover, current anti-allergic therapies still have problems such as varied efficacy among individual patient and high medical expenses. Those situations strongly suggest a necessity for the development of safer and more effective strategies for intervention of allergic disorders. In the present study, I aimed to explore novel allergy preventive and therapeutic molecules upon targeting IgE-mediated mast cell response.

In Chapter 1, I demonstrated that endogenous histone H1 acted as a novel danger signal upon allergy exacerbation. Serum histone H1 levels elevated in OVA-immunized mice. In these mice, nasal sensitization alone with histone H1 (even without OVA) showed a significant exacerbation of nasal symptoms and mast cell infiltration into nasal mucosa. Additionally, histone H1 even without antigen induced degranulation as well as production of autocrine factor IL-6 from IgE-sensitized mast cells. Moreover, endogenous histone H1 was secreted with antigen-induced degranulation from mast cells. Finally, histone H1 exacerbated mast cell-dependent allergic inflammation in PCA model mice. Those results suggested that disturbance of endogenous histone H1-mediated positive feedback loop of mast cell degranulation may be a useful strategy for therapy of allergic disorders.

In Chapter 2, I demonstrated the therapeutic potency of histone H1-targeted monoclonal antibody, SSV mAb, against type I allergic disorders. SSV mAb showed a significant suppression of antigen-induced degranulation from IgE-sensitized mast cells. Moreover, SSV mAb significantly ameliorated allergic rhinitis without affecting systemic immune responses, suggesting that the SSV mAb therapy specifically acts on the IgE-mast cell axis to fulfill its anti-allergic activity.

In Chapter 3, I discovered a novel potent anti-allergic compound, 8-hydroxy-5,7-dimethoxyflavanone, referred to *Perilla*-derived methoxyflavanone (PDMF). The allergy preventive potency of PDMF was more prominent than those of the known *P. frutescens*-derived anti-inflammatory polyphenols, as demonstrated by *in vitro* and *in vivo* mast cell degranulation reaction models as well as by a murine model of Japanese cedar pollinosis. I also found that PDMF acts on FcεRI-dependent signal transduction pathway to fulfill its anti-allergic potency, in which PDMF suppressed Akt-activation and intracellular Ca^{2+} influx. Since Akt up-regulates mast cell granule translocation and Ca^{2+} influx is essential for granule exocytosis, PDMF inhibits both pathways critical for mast cell degranulation.

The present study shows a novel pathogenic mechanism of mast cell-driven type I allergy, in which endogenous histone H1 acts on mast cells to exacerbate allergic inflammation. I also demonstrate endogenous histone H1 is a useful therapeutic target for type I allergy. Additionally, I discover a

novel flavanone-derivative form the Asian medicinal herb *P. frutescens* (PDMF), which would be useful for preventive medicine and/or food factor regulation of allergic disorders. These thesis study represents novel strategies for prevention and therapy for mast cell-mediated allergic disorders. I strongly hope that the study direct development of safety and effective strategy for allergic disorders as refractory disease.

Acknowledgements

This thesis study has been carried out at the Molecular Biochemistry Lab., Department of Molecular Biotechnology, Graduate School of Advanced Sciences of Matter, Hiroshima University. First of all, I present special thanks and respects for Prof. Seiji Kawamoto. I am grateful to Prof. Tsunehiro Aki, Prof. Kenji Arakawa and Prof. Junichi Kato, they advised for my doctoral thesis and judged it as a reviewer. I was always helped by Prof. Takashi Fujimura, and Prof. Kazuhisa Ono (Faculty of Life Sciences, Hiroshima Institute of Technology, Japan), their directions and encouragements became the root of my studies as well as their ideas and coaching was essential for my works. Prof. Miyako Nakano is also the important commentator for my works.

Chapter 1 and 2 are collaborated studies with four institutes (Graduate Institute of Clinical Medical Sciences, Chang Gung University College of Medicine, Taiwan. Liver Transplantation Program and Division of Transplant Immunology, Institute for Translational Research in Biomedical Sciences, Kaohsiung Chang Gung Memorial Hospital, Taiwan. Kazusa Institute for Drug Discovery and Faculty of Nursing, Josai International University, Japan). I am grateful to Prof. Toshiaki Nakano and Yuki Takaoka Ph.D., their idea and critical data such as allergic rhinitis model became foundation of those chapters. I could never complete

my thesis without advises and efforts of the members belonging to the above collaborated institutes. Especially, Ms. Aiko Teshima and Ms. Akane Hori supported well my works.

Chapter 2 is a collaborated study with Mishima Foods Co. Ltd., Japan, and constructed mainly by their foundation and *P. frutescens* dry leaves. I deeply thank Ms. Noriko Hirakawa and Mr. Kenji Baba for lots of encouragements and advice. I really appreciate that Prof. Kenji Arakawa helped structural analyses of PDMF and advised my published paper. I am grateful to Ms. Tomoko Amimoto (the Natural Science Center for Basic Research and Development (N-BARD), Hiroshima University), she helped MS analyses using LTQ Orbitrap XL mass spectrometer with APCI method. Prof. Yohsuke Ooyama (Hiroshima University) helped FT-IR spectra analyses on GladiATR10. I think Ms. Miki Matsuda is an essential person for the mechanical analyses of PDMF.

I could never finish my works without lots of help for discussions and encouragements by my laboratory members. Finally, I present special thanks to my family, their heart-worming supports always relieved and encouraged me. I would like to return those favors.

References

1 Weinberg, E. G. The WAO white book on allergy 2011-2012. *Current Allergy & Clinical Immunology* **24**, 156-157 (2011).

2 de Jong, E. C., Vieira, P. L., Kalinski, P., Schuitemaker, J. H., Tanaka, Y., Wierenga, E. A., Yazdanbakhsh, M. and Kapsenberg, M. L. Microbial compounds selectively induce Th1 cell-promoting or Th2 cell-promoting dendritic cells in vitro with diverse th cell-polarizing signals. *Journal of Immunology* **168**, 1704-1709 (2002).

3 Rengarajan, J., Szabo, S. J. and Glimcher, L. H. Transcriptional regulation of Th1/Th2 polarization. *Immunology Today* **21**, 479-483 (2000).

4 Takeuchi, O. and Akira, S. Pattern recognition receptors and inflammation. *Cell* **140**, 805-820 (2010).

5 Anders, H. J. and Schaefer, L. Beyond Tissue injury-damage-associated molecular patterns, toll-like receptors, and inflammasomes also drive regeneration and fibrosis. *Journal of the American Society of Nephrology* **25**, 1387-1400 (2014).

6 Matsushita, K., Kato, Y., Akasaki, S. and Yoshimoto, T. Proallergic cytokines and group 2 innate lymphoid cells in allergic nasal diseases. *Allergollogy International* **64**, 235-240 (2015).

7 Galli, S. J. and Tsai, M. IgE and mast cells in allergic disease. *Nature Medicine* **18**, 693-704 (2012).

8 Pejler, G., Abrink, M., Ringvall, M. and Wernersson, S. Mast cell proteases. *Advances in Immunology* **95**, 167-255 (2007).

9 Theoharides, T. C., Singh, L. K., Boucher, W., Pang, X. Z., Letourneau, R., Webster, E. and Chrousos, G. Corticotropin-releasing hormone induces skin mast cell degranulation and increased vascular permeability, a possible explanation for its proinflammatory effects.

Endocrinology **139**, 403-413 (1998).

10 Weltman, J. K. Update on histamine as a mediator of inflammation. *Allergy and Asthma Proceedings* **21**, 334-334 (2000).

11 Haas, H. L., Sergeeva, O. A. and Selbach, O. Histamine in the nervous system. *Physiology Review* **88**, 1183-1241 (2008).

12 Kitawaki, T., Kadowaki, N., Sugimoto, N., Kambe, N., Hori, T., Miyachi, Y., Nakahata, T. and Uchiyama, T. IgE-activated mast cells in combination with pro-inflammatory factors induce Th2-promoting dendritic cells. *International Immunology* **18**, 1789-1799 (2006).

13 Xue, L., Salimi, M., Panse, I., Mjosberg, J. M., McKenzie, A. N., Spits, H., Klenerman, P. and Ogg, G. Prostaglandin D2 activates group 2 innate lymphoid cells through chemoattractant receptor-homologous molecule expressed on Th2 cells. *Journal of Allergy and Clinical Immunology* **133**, 1184-1194 (2014).

14 Hart, P. H. Regulation of the inflammatory response in asthma by mast cell products. *Immunology and Cell Biology* **79**, 149-153 (2001).

15 Halim, T. Y., Krauss, R. H., Sun, A. C. and Takei, F. Lung natural helper cells are a critical source of Th2 cell-type cytokines in protease allergen-induced airway inflammation. *Immunity* **36**, 451-463 (2012).

16 Louten, J., Rankin, A. L., Li, Y., Murphy, E. E., Beaumont, M., Moon, C., Bourne, P., McClanahan, T. K., Pflanz, S. and de Waal Malefyt, R. Endogenous IL-33 enhances Th2 cytokine production and T-cell responses during allergic airway inflammation. *International Immunology* **23**, 307-315 (2011).

17 Haenuki, Y., Matsushita, K., Futatsugi-Yumikura, S., Ishii, K. J., Kawagoe, T., Imoto, Y., Fujieda, S., Yasuda, M., Hisa, Y., Akira, S., Nakanishi, K. and Yoshimoto, T. A critical role of IL-33 in experimental allergic rhinitis. *Journal of Allergy and Clinical Immunology* **130**, 184-194 e111 (2012).

18 Ying, S., O'Connor, B., Ratoff, J., Meng, Q., Mallett, K., Cousins, D.,

Robinson, D., Zhang, G. Z., Zhao, J. S., Lee, T. H. and Corrigan, C. Thymic stromal lymphopoietin expression is increased in asthmatic airways and correlates with expression of TH2-attracting chemokines and disease severity. *Journal of Immunology* **174**, 8183-8190 (2005).

19 Wang, Y. H., Angkasekwinai, P., Lu, N., Voo, K. S., Arima, K., Hanabuchi, S., Hippe, A., Corrigan, C. J., Dong, C., Homey, B., Yao, Z., Ying, S., Huston, D. P. and Liu, Y. J. IL-25 augments type 2 immune responses by enhancing the expansion and functions of TSLP-DC-activated Th2 memory cells. *Journal of Experimental Medicine* **204**, 1837-1847 (2007).

20 Han, N. R., Oh, H. A., Nam, S. Y., Moon, P. D., Kim, D. W., Kim, H. M. and Jeong, H. J. TSLP induces mast cell development and aggravates allergic reactions through the activation of MDM2 and STAT6. *Journal of Investigative Dermatology* **134**, 2521-2530 (2014).

21 Palmer, H. S., Kelso, E. B., Lockhart, J. C., Sommerhoff, C. P., Plevin, R., Goh, F. G. and Ferrell, W. R. Protease-activated receptor 2 mediates the proinflammatory effects of synovial mast cells. *Arthritis and Rheumatism* **56**, 3532-3540 (2007).

22 Sawaguchi, M., Tanaka, S., Nakatani, Y., Harada, Y., Mukai, K., Matsunaga, Y., Ishiwata, K., Oboki, K., Kambayashi, T., Watanabe, N., Karasuyama, H., Nakae, S., Inoue, H. and Kubo, M. Role of mast cells and basophils in IgE responses and in allergic airway hyperresponsiveness. *Journal of Immunology* **188**, 1809-1818 (2012).

23 McNeil, B. D., Pundir, P., Meeker, S., Han, L., Undem, B. J., Kulka, M. and Dong, X. Identification of a mast-cell-specific receptor crucial for pseudo-allergic drug reactions. *Nature* **519**, 237-241 (2015).

24 Tatemoto, K., Nozaki, Y., Tsuda, R., Konno, S., Tomura, K., Furuno, M., Ogasawara, H., Edamura, K., Takagi, H., Iwamura, H., Noguchi, M. and Naito, T. Immunoglobulin E-independent activation of mast cell is mediated by Mrg receptors. *Biochemical and Biophysical*

Research Communications **349**, 1322-1328 (2006).

25 Gilfillan, A. M. and Tkaczyk, C. Integrated signalling pathways for mast-cell activation. *Nature Reviews: Immunology* **6**, 218-230 (2006).

26 Baram, D., Linial, M., Mekori, Y. A. and Sagi-Eisenberg, R. Cutting edge: Ca^{2+}-dependent exocytosis in mast cells is stimulated by the Ca^{2+} sensor, synaptotagmin. *Journal of Immunology* **161**, 5120-5123 (1998).

27 Kawakami, Y., Nishimoto, H., Kitaura, J., Maeda-Yamamoto, M., Kato, R. M., Littman, D. R., Leitges, M., Rawlings, D. J. and Kawakami, T. Protein kinase C beta II regulates Akt phosphorylation on Ser-473 in a cell type- and stimulus-specific fashion. *Journal of Biological Chemistry* **280**, 8628-8628 (2005).

28 Bousquet, J., Lockey, R., Malling, H. J. and members, W. p. Allergen immunotherapy: Therapeutic vaccines for allergic diseases - A WHO position paper. *Journal of Allergy and Clinical Immunology* **102**, 558-562 (1998).

29 Valenta, R. The future of antigen-specific immunotherapy of allergy. *Nature Reviews: Immunology* **2**, 446-453 (2002).

30 Akdis, M. and Akdis, C. A. Mechanisms of allergen-specific immunotherapy: Multiple suppressor factors at work in immune tolerance to allergens. *Journal of Allergy and Clinical Immunology* **133**, 621-631 (2014).

31 James, L. K. and Till, S. J. Potential mechanisms for IgG4 inhibition of immediate hypersensitivity reactions. *Current Allergy and Asthma Reports* **16**, 23 (2016).

32 Valenta, R., Lidholm, J., Niederberger, V., Hayek, B., Kraft, D. and Gronlund, H. The recombinant allergen-based concept of component-resolved diagnostics and immunotherapy (CRD and CRIT). *Clinical and Experimental Allergy* **29**, 896-904 (1999).

33 Okamoto Y, F. S., Ota N, Okano M, Kamijo A, Goto M, Suzuki M,

Takeno Y, Terada T, Hanazawa T, Horiguchi S, Honda K, Matsune A, Yamada T, Yuda A, and Nakayama T. A guide to immunotherapy for allergic rhinitis. *Nihon Bika Gakkai Kaishi (Japanese Journal of Rhinology)* **51**, 119-154 (2012).

34 Nagai, H. Prostaglandin as a target molecule for pharmacotherapy of allergic inflammatory diseases. *Allergology International* **57**, 187-196 (2008).

35 Chang, T. W., Wu, P. C., Hsu, C. L. and Hung, A. F. Anti-IgE antibodies for the treatment of IgE-mediated allergic diseases. *Advances in Immunology* **93**, 63-119 (2007).

36 Mauser, P. J., Pitman, A., Witt, A., Fernandez, X., Zurcher, J., Kung, T., Jones, H., Watnick, A. S., Egan, R. W. and Kreutner, W. Inhibitory effect of the TRFK-5 anti-IL-5 antibody in a guinea pig model of asthma. *American Review of Respiratory Disease* **148**, 1623-1627 (1993).

37 Smith, D. A., Minthorn, E. A. and Beerahee, M. Pharmacokinetics and pharmacodynamics of mepolizumab, an anti-interleukin-5 monoclonal antibody. *Clinical Pharmacokinetics* **50**, 215-227 (2011).

38 Patterson, C. and Chambers, L. W. Preventive health-care. *Lancet* **345**, 1611-1615 (1995).

39 Mokdad, A. H., Marks, J. S., Stroup, D. F. and Gerberding, J. L. Actual causes of death in the United States, 2000. *JAMA* **291**, 1238-1245 (2004).

40 Swinbanks, D. and Obrien, J. Japan explores the boundary between food and medicine. *Nature* **364**, 180-180 (1993).

41 Wei, D., Ci, X., Chu, X., Wei, M., Hua, S. and Deng, X. Hesperidin suppresses ovalbumin-induced airway inflammation in a mouse allergic asthma model. *Inflammation* **35**, 114-121 (2012).

42 Maeda-Yamamoto, M., Ema, K. and Shibuichi, I. *In vitro* and *in vivo* anti-allergic effects of 'benifuuki' green tea containing O-methylated

catechin and ginger extract enhancement. *Cytotechnology* **55**, 135-142 (2007).

43 Shida, K., Takahashi, R., Iwadate, E., Takamizawa, K., Yasui, H., Sato, T., Habu, S., Hachimura, S. and Kaminogawa, *S. Lactobacillus casei* strain Shirota suppresses serum immunoglobulin E and immunoglobulin G1 responses and systemic anaphylaxis in a food allergy model. *Clinical and Experimental Allergy* **32**, 563-570 (2002).

44 Ishida, Y., Nakamura, F., Kanzato, H., Sawada, D., Yamamoto, N., Kagata, H., Oh-Ida, M., Takeuchi, H. and Fujiwara, S. Effect of milk fermented with *Lactobacillus acidophilus* strain L-92 on symptoms of Japanese cedar pollen allergy: a randomized placebo-controlled trial. *Bioscience, Biotechnology, and Biochemistry* **69**, 1652-1660 (2005).

45 Martins, I., Wang, Y., Michaud, M., Ma, Y., Sukkurwala, A. Q., Shen, S., Kepp, O., Metivier, D., Galluzzi, L., Perfettini, J. L., Zitvogel, L. and Kroemer, G. Molecular mechanisms of ATP secretion during immunogenic cell death. *Cell Death and Differentiation* **21**, 79-91 (2014).

46 Bours, M. J., Dagnelie, P. C., Giuliani, A. L., Wesselius, A. and Di Virgilio, F. P2 receptors and extracellular ATP: a novel homeostatic pathway in inflammation. *Frontiers in Bioscience (Scholar Edition)* **3**, 1443-1456 (2011).

47 Panther, E., Corinti, S., Idzko, M., Herouy, Y., Napp, M., la Sala, A., Girolomoni, G. and Norgauer, J. Adenosine affects expression of membrane molecules, cytokine and chemokine release, and the T-cell stimulatory capacity of human dendritic cells. *Blood* **101**, 3985-3990 (2003).

48 Kurashima, Y. and Kiyono, H. New era for mucosal mast cells: their roles in inflammation, allergic immune responses and adjuvant development. *Experimental and Molecular Medicine* **46** (2014).

49 Schulman, E. S., Glaum, M. C., Post, T., Wang, Y., Raible, D. G.,

Mohanty, J., Butterfield, J. H. and Pelleg, A. ATP modulates anti-IgE-induced release of histamine from human lung mast cells. *American Journal of Respiratory Cell and Molecular Biology* **20**, 530-537 (1999).

50 Ekaney, M. L., Otto, G. P., Sossdorf, M., Sponholz, C., Boehringer, M., Loesche, W., Rittirsch, D., Wilharm, A., Kurzai, O., Bauer, M. and Claus, R. A. Impact of plasma histones in human sepsis and their contribution to cellular injury and inflammation. *Critical Care* **18** (2014).

51 Sagi-Eisenberg, R., Foreman, J. C. and Shelly, R. Histamine release induced by histone and phorbol ester from rat peritoneal mast cells. *European Journal of Pharmacology* **113**, 11-17 (1985).

52 Kusano, T., Chiang, K. C., Inomata, M., Shimada, Y., Ohmori, N., Goto, T., Sato, S., Goto, S., Nakano, T., Kawamoto, S., Takaoka, Y., Shiraishi, N., Noguchi, T. and Kitano, S. A novel anti-histone H1 monoclonal antibody, SSV monoclonal antibody, improves lung injury and survival in a mouse model of lipopolysaccharide-induced sepsis-like syndrome. *Biomed Research International* **2015**, 491649 (2015).

53 Nakano, T., Goto, S., Lai, C. Y., Hsu, L. W., Wong, J. L., Kawamoto, S., Chiang, K. C., Ohmori, N., Goto, T., Sato, S., Yang, C. H., Wang, C. C., Jawan, B., Cheng, Y. F., Ono, K. and Chen, C. L. Involvement of autoimmunity against nuclear histone H1 in liver transplantation tolerance. *Transplant Immunology* **19**, 87-92 (2008).

54 Kumar, V. and Sharma, A. Mast cells: emerging sentinel innate immune cells with diverse role in immunity. *Molecular Immunology* **48**, 14-25 (2010).

55 Jungraithmayr, W. The putative role of mast cells in lung transplantation. *American Journal of Transplantation* **15**, 594-600 (2015).

56 Miyahara, S., Miyahara, N., Takeda, K., Joetham, A. and Gelfand, E. W. Physiologic assessment of allergic rhinitis in mice: role of the high-affinity IgE receptor (FcepsilonRI). *Journal of Allergy and Clinical Immunology* **116**, 1020-1027 (2005).

57 Onishi, N., Kawamoto, S., Ueda, K., Yamanaka, Y., Katayama, A., Suzuki, H., Aki, T., Hashimoto, K., Hide, M. and Ono, K. Dietary pulverized konjac glucomannan prevents the development of allergic rhinitis-like symptoms and IgE response in mice. *Bioscience, Biotechnology, and Biochemistry* **71**, 2551-2556 (2007).

58 Nakano, T., Chen, C. L. and Goto, S. Nuclear antigens and auto/alloantibody responses: friend or foe in transplant immunology. *Clinical and Developmental Immunology* **2013**, 267156 (2013).

59 Nakano, T., Goto, S., Lai, C. Y., Hsu, L. W., Tseng, H. P., Chen, K. D., Chiu, K. W., Wang, C. C., Cheng, Y. F. and Chen, C. L. Induction of antinuclear antibodies by de novo autoimmune hepatitis regulates alloimmune responses in rat liver transplantation. *Clinical and Developmental Immunology* **2013**, 413928 (2013).

60 Guibas, G. V., Lakis, S., Gkimpas, C., Manda, M., Kapoukranidou, D. and Spandou, E. Efficiency of different decalcification protocols for nasal osseous structures in a rat experimental model of allergic rhinitis, and their effects on epithelial histology: an attempt at standardization. *Experimental and Toxicologic Pathology* **66**, 469-475 (2014).

61 Seldin, D. C., Adelman, S., Austen, K. F., Stevens, R. L., Hein, A., Caulfield, J. P. and Woodbury, R. G. Homology of the rat basophilic leukemia cell and the rat mucosal mast cell. *Proceedings of the National Academy of Sciences of the United States of America* **82**, 3871-3875 (1985).

62 Nakano, T., Lai, C. Y., Goto, S., Hsu, L. W., Kawamoto, S., Ono, K., Chen, K. D., Lin, C. C., Chiu, K. W., Wang, C. C., Cheng, Y. F. and

Chen, C. L. Immunological and regenerative aspects of hepatic mast cells in liver allograft rejection and tolerance. *PLoS ONE* **7**, e37202 (2012).

63 Silwal, P., Shin, K., Choi, S., Kang, S. W., Park, J. B., Lee, H. J., Koo, S. J., Chung, K. H., Namgung, U., Lim, K., Heo, J. Y., Park, J. I. and Park, S. K. Adenine suppresses IgE-mediated mast cell activation. *Molecular Immunology* **65**, 242-249 (2015).

64 von Kockritz-Blickwede, M., Goldmann, O., Thulin, P., Heinemann, K., Norrby-Teglund, A., Rohde, M. and Medina, E. Phagocytosis-independent antimicrobial activity of mast cells by means of extracellular trap formation. *Blood* **111**, 3070-3080 (2008).

65 Mishra, B., von der Ohe, M., Schulze, C., Bian, S., Makhina, T., Loers, G., Kleene, R. and Schachner, M. Functional role of the interaction between polysialic acid and extracellular histone H1. *Journal of Neuroscience* **30**, 12400-12413 (2010).

66 Hsu, L. W., Chen, C. L., Nakano, T., Lai, C. Y., Chiang, K. C., Lin, Y. C., Kao, Y. H., Chen, S. H., Goto, T., Sung, W. C., Yang, C. H., Cheng, Y. F., Jawan, B., Chiu, K. W. and Goto, S. The role of a nuclear protein, histone H1, on signalling pathways for the maturation of dendritic cells. *Clinical and Experimental Immunology* **152**, 576-584 (2008).

67 Oskeritzian, C. A., Zhao, W., Pozez, A. L., Cohen, N. M., Grimes, M. and Schwartz, L. B. Neutralizing endogenous IL-6 renders mast cells of the MCT type from lung, but not the MCTc type from skin and lung, susceptible to human recombinant IL-4-induced apoptosis. *Journal of Immunology* **172**, 593-600 (2004).

68 Genovese, A., Borgia, G., Bouvet, J. P., Detoraki, A., de Paulis, A., Piazza, M. and Marone, G. Protein Fv produced during viral hepatitis is an endogenous immunoglobulin superantigen activating human heart mast cells. *International Archives of Allergy and Immunology*

132, 336-345 (2003).

69 Tasaka, K., Mio, M., Akagi, M. and Saito, T. Histamine release induced by histone and related morphological changes in mast cells. *Agents and Actions* **30**, 114-117 (1990).

70 Fujisawa, D., Kashiwakura, J., Kita, H., Kikukawa, Y., Fujitani, Y., Sasaki-Sakamoto, T., Kuroda, K., Nunomura, S., Hayama, K., Terui, T., Ra, C. and Okayama, Y. Expression of Mas-related gene X2 on mast cells is upregulated in the skin of patients with severe chronic urticaria. *Journal of Allergy and Clinical Immunology* **134**, 622-+ (2014).

71 Nakano, T., Kawamoto, S., Lai, C. Y., Sasaki, T., Aki, T., Shigeta, S., Goto, T., Sato, S., Goto, S., Chen, C. L. and Ono, K. Liver transplantation-induced antihistone H1 autoantibodies suppress mixed lymphocyte reaction. *Transplantation* **77**, 1595-1603 (2004).

72 Chiang, K. C., Shimada, Y., Nakano, T., Lai, C. Y., Hsu, L. W., Goto, S., Ohmori, N., Mori, K., Miyagi, T., Kawamoto, S., Ono, K., Chen, C. L., Goto, T. and Sato, S. A novel peptide mimotope identified as a potential immunosuppressive vaccine for organ transplantation. *Journal of Immunology* **182**, 4282-4288 (2009).

73 Kusano, T., Chiang, K.-C., Inomata, M., Shimada, Y., Ohmori, N., Goto, T., Sato, S., Goto, S., Nakano, T., Kawamoto, S., Takaoka, Y., Shiraishi, N., Noguchi, T. and Kitano, S. A novel anti-histone H1 monoclonal antibody, SSV monoclonal antibody, improves lung injury and survival in a mouse model of lipopolysaccharide-induced sepsis-like syndrome. *BioMed Research International* **2015**, 10 (2015).

74 Oh, H. A., Park, C. S., Ahn, H. J., Park, Y. S. and Kim, H. M. Effect of *Perilla frutescens var. acuta Kudo* and rosmarinic acid on allergic inflammatory reactions. *Experimental Biology and Medicine (Maywood, N.J.)* **236**, 99-106 (2011).

75 Takano, H., Osakabe, N., Sanbongi, C., Yanagisawa, R., Inoue, K.,

Yasuda, A., Natsume, M., Baba, S., Ichiishi, E. and Yoshikawa, T. Extract of *Perilla frutescens* enriched for rosmarinic acid, a polyphenolic phytochemical, inhibits seasonal allergic rhinoconjunctivitis in humans. *Experimental Biology and Medicine (Maywood, N.J.)* **229**, 247-254 (2004).

76 Watson, R. R., Preedy, V. R. and Zibadi, S. *Polyphenols in human health and disease*. (Elsevier/Academic Press, 2014).

77 Asif, M. Phytochemical study of polyphenols in *Perilla frutescens* as an antioxidant. *Avicenna J Phytomed* **2**, 169-178 (2012).

78 Sanbongi, C., Takano, H., Osakabe, N., Sasa, N., Natsume, M., Yanagisawa, R., Inoue, K. I., Sadakane, K., Ichinose, T. and Yoshikawa, T. Rosmarinic acid in *Perilla* extract inhibits allergic inflammation induced by mite allergen, in a mouse model. *Clinical and Experimental Allergy* **34**, 971-977 (2004).

79 Hossen, M. A., Inoue, T., Shinmei, Y., Minami, K., Fujii, Y. and Kamei, C. Caffeic acid inhibits compound 48/80-induced allergic symptoms in mice. *Biological and Pharmaceutical Bulletin* **29**, 64-66 (2006).

80 Jeon, I. H., Kim, H. S., Kang, H. J., Lee, H. S., Jeong, S. I., Kim, S. J. and Jang, S. I. Anti-inflammatory and antipruritic effects of luteolin from *Perilla* (*P. frutescens L.*) leaves. *Molecules* **19**, 6941-6951 (2014).

81 Ueda, H., Yamazaki, C. and Yamazaki, M. Luteolin as an anti-inflammatory and anti-allergic constituent of *Perilla frutescens*. *Biological and Pharmaceutical Bulletin* **25**, 1197-1202 (2002).

82 Yano, S., Umeda, D., Yamashita, S., Yamada, K. and Tachibana, H. Dietary apigenin attenuates the development of atopic dermatitis-like skin lesions in NC/Nga mice. *The Journal of Nutritional Biochemistry* **20**, 876-881 (2009).

83 Segal, D. M., Taurog, J. D. and Metzger, H. Dimeric immunoglobulin-E serves as a unit signal for mast-cell degranulation.

Proceedings of the National Academy of Sciences of the United States of America **74**, 2993-2997 (1977).

84 Ishizaka, T. The Robert A. Cooke memorial lecture. Analysis of triggering events in mast cells for immunoglobulin E-mediated histamine release. *Journal of Allergy and Clinical Immunology* **67**, 90-96 (1981).

85 Lewis, R. A., Soter, N. A., Diamond, P. T., Austen, K. F., Oates, J. A. and Roberts, L. J., 2nd. Prostaglandin D2 generation after activation of rat and human mast cells with anti-IgE. *Journal of Immunology* **129**, 1627-1631 (1982).

86 Kraft, S. and Kinet, J. P. New developments in Fc epsilon RI regulation, function and inhibition. *Nature Reviews Immunology* **7**, 365-378 (2007).

87 Tang, K. S., Konczak, I. and Zhao, J. Identification and quantification of phenolics in Australian native mint (*Mentha australis R. Br.*). *Food Chemistry* **192**, 698-705 (2016).

88 Oishi, T., Tanaka, K. I., Hashimoto, T., Shinbo, Y., Jumtee, K., Bamba, T., Fukusaki, E., Suzuki, H., Shibata, D., Takahashi, H., Asahi, H., Kurokawa, K., Nakamura, Y., Hirai, A., Nakamura, K., Altaf-Ul-Amin, M. and Kanaya, S. An approach to peak detection in GC-MS chromatograms and application of KNApSAcK database in prediction of candidate metabolites. *Plant Biotechnology* **26**, 167-174 (2009).

89 Gee, K. R., Brown, K. A., Chen, W. N., Bishop-Stewart, J., Gray, D. and Johnson, I. Chemical and physiological characterization of fluo-4 Ca^{2+}-indicator dyes. *Cell Calcium* **27**, 97-106 (2000).

90 Tsujimura, T., Furitsu, T., Morimoto, M., Kanayama, Y., Nomura, S., Matsuzawa, Y., Kitamura, Y. and Kanakura, Y. Substitution of an aspartic acid results in constitutive activation of c-kit receptor tyrosine kinase in a rat tumor mast cell line RBL-2H3. *International*

Archives of Allergy and Immunology **106**, 377-385 (1995).

91 Wilson, B. S., Pfeiffer, J. R. and Oliver, J. M. Fc epsilon RI signaling observed from the inside of the mast cell membrane. *Molecular Immunology* **38**, 1259-1268 (2002).

92 Asada, M., Fukumori, Y., Inoue, M., Nakagomi, K., Sugie, M., Fujita, Y., Tomizuka, N., Yamazaki, Y. and Oka, S. Glycoprotein derived from the hot water extract of mint plant, *Perilla frutescens britton*. *J Agric Food Chem* **47**, 468-472 (1999).

93 Toda, S., Kimura, M., Ohnishi, M. and Nakashima, K. Effects of the Chinese herbal medicine "saiboku-to" on histamine release from and the degranulation of mouse peritoneal mast cells induced by compound 48/80. *Journal of Ethnopharmacology* **24**, 303-309 (1988).

94 Gaggeri, R., Rossi, D., Christodoulou, M. S., Passarella, D., Leoni, F., Azzolina, O. and Collina, S. Chiral flavanones from *Amygdalus lycioides Spach*: structural elucidation and identification of TNFalpha inhibitors by bioactivity-guided fractionation. *Molecules* **17**, 1665-1674 (2012).

95 Hughes, R. J., Croley, T. R., Metcalfe, C. D. and March, R. E. A tandem mass spectrometric study of selected characteristic flavonoids. *International Journal of Mass Spectrometry* **210**, 371-385 (2001).

96 Vieira, P. C., Dealvarenga, M. A., Gottlieb, O. R. and Gottlieb, H. E. 4-Hexadecenylphenol and flavonoids from *Piper hispidum*. *Planta Medica* **39**, 153-156 (1980).

97 Nakajima, A., Yamamoto, Y., Yoshinaka, N., Namba, M., Matsuo, H., Okuyama, T., Yoshigai, E., Okumura, T., Nishizawa, M. and Ikeya, Y. A new flavanone and other flavonoids from green *Perilla* leaf extract inhibit nitric oxide production in interleukin 1 beta-treated hepatocytes. *Bioscience Biotechnology and Biochemistry* **79**, 138-146 (2015).

98 Kawamura, H., Mishima, K., Sharmin, T., Ito, S., Kawakami, R.,

Kato, T., Misumi, M., Suetsugu, T., Orii, H., Kawano, H., Irie, K., Sano, K., Mishima, K., Harada, T., Mustofa, S., Hasanah, F., Siregar, Y. D., Zahroh, H., Putri, L. S. and Salim, A. Ultrasonically enhanced extraction of luteolin and apigenin from the leaves of *Perilla frutescens* (*L.*) *Britt.* using liquid carbon dioxide and ethanol. *Ultrasonics Sonochemistry* **29**, 19-26 (2016).

99 Mastuda, H., Morikawa, T., Ueda, K., Managi, H. and Yoshikawa, M. Structural requirements of flavonoids for inhibition of antigen-induced degranulation, TNF-alpha and IL-4 production from RBL-2H3 cells. *Bioorganic and Medicinal Chemistry* **10**, 3123-3128 (2002).

100 Shichijo, M., Yamamoto, N., Tsujishita, H., Kimata, M., Nagai, H. and Kokubo, T. Inhibition of syk activity and degranulation of human mast cells by flavonoids. *Biological and Pharmaceutical Bulletin* **26**, 1685-1690 (2003).

101 Murata, K., Takano, S., Masuda, M., Iinuma, M. and Matsuda, H. Anti-degranulating activity in rat basophil leukemia RBL-2H3 cells of flavanone glycosides and their aglycones in citrus fruits. *Journal of Natural Medicines* **67**, 643-646 (2013).

102 Kim, M. S., Radinger, M. and Gilfillan, A. M. The multiple roles of phosphoinositide 3-kinase in mast cell biology. *Trends in Immunology* **29**, 493-501 (2008).

103 Yoo, J. M., Kim, J. H., Park, S. J., Kang, Y. J. and Kim, T. J. Inhibitory effect of eriodictyol on IgE/Ag-induced type I hypersensitivity. *Bioscience, Biotechnology, and Biochemistry* **76**, 1285-1290 (2012).

公表論文

(1) Impact of histone H1 on the progression of allergic rhinitis and its suppression by neutralizing antibody in mice
Toshiaki Nakano, Rikiya Kamei, Takashi Fujimura, Yuki Takaoka, Ayane Hori, Chia-Yun Lai, Kuei-Chen Chiang, Yayoi Shimada, Naoya Ohmori, Takeshi Goto, Kazuhisa Ono, Chao-Long Chen, Shigeru Goto, and Seiji Kawamoto
PLoS ONE, **11** (4), e0153630 (2016) (19 pages)

(2) A flavanone derivative from the Asian medicinal herb (*Perilla frutescens*) potently suppresses IgE-mediated immediate hypersensitivity reactions.
Rikiya Kamei, Takashi Fujimura, Miki Matsuda, Kotaro Kakihara, Noriko Hirakawa, Kenji Baba, Kazuhisa Ono, Kenji Arakawa, and Seiji Kawamoto.
Biochemical and Biophysical Research Communications, 483, 674-679 (2017)